Simulation and control of a small scale sodium sulphate salt splitting plant

JF Bijzet


orcid.org/0000-0003-4612-1628

Dissertation graduation in fulfilment of the requirements for the degree *Master of Engineering Chemical Engineering* at the North-West University

Supervisor:	Prof Q Campbell
Co-supervisors:	Prof OSL Bruinsma
	Prof DJ Branken

Graduation:	May 2022
Student number:	27115240

ACKNOWLEDGEMENTS

Foremost, I would like to thank Arxo Metals, without whom this project would not be possible. I will forever be grateful for the contribution they made to my career in Chemical Engineering.

To my supervisor, Professor Quentin Campbell, thank you for your words of affirmation and the frequent proofreading of my dissertation. Your motivation made me feel confident in producing a dissertation on time and of good quality.

Professor Dolf Bruinsma, I would like to thank you for your continuous support and guidance, as well as the vast amount of knowledge you contributed to this study. I could not have asked for a better advisor and mentor.

I would also like to express my appreciation to Professor Dawie Branken for your time and insight throughout the project.

I am extremely grateful to my parents for their love, prayers, caring and sacrifices. Thank you for investing in my future. And to Marisha Gordon, your love, patience and unwavering support supplied me with the willpower to push through the hard times and never give up.

“A smooth sea never made a skilled sailor.”

- Franklin D. Roosevelt

ABSTRACT

Base metal refineries produce sodium sulphate solutions as a waste product in the precipitation step. The solution that is formed generally has a concentration of around 100 g Na_2SO_4/L. Discharging solutions with such high concentrations into the environment can upset the biodiversity of nearby water sources due to its high salinity and, thus, the solution should be treated. Currently, the most widely used treatment method is evaporative crystallisation. Evaporative crystallisation produces potable water, but the large capital cost, high energy consumption and the production of a salt with low to zero economic value establish the need for a better alternative.

A continuous electrodialysis with bipolar membranes integrated with disc reverse osmosis setup was designed, built and used to treat a sodium sulphate solution to produce potable water, sodium hydroxide and sulphuric acid. The study aimed to develop a process with a robust control system and to minimise the production cost of sodium hydroxide via manipulation of the salt concentration, temperature and current density.

The salt concentration, temperature, current density and flow rates were varied to determine their effects on the performance of the setup. The control system was able to keep the parameters at their respective setpoints throughout an experiment. Circulation flowrate tests showed that mass transfer limitations were negligible at the high flow rates used in this study. A maximum salt splitting rate of 1.08 kg/h/m^2 at a power density of 1.76 kW/m^2 was found, as well as a minimum specific energy consumption of 3.19 kWh/kg at a power density of 1.81 kW/m^2. The sodium hydroxide and sulphuric acid produced had concentrations of 66.5 g/L and 53.7 g/L and purities of 90.5% and 74% respectively, with sodium sulphate being the main impurity in both cases. The lowest cost to produce sodium hydroxide, accounting for equipment cost, operational cost and electricity usage was found to be €0.78/kg at a sodium sulphate concentration of 150 g/L, an operating temperature of 35°C and a power density of 1.81 kW/m^2.

Using these results, together with a fair cost analysis for each individual case, a decision can be made whether it is economically viable to use electrodialysis with bipolar membranes integrated with disc reverse osmosis to treat a sodium sulphate waste stream.

Key words: Salt splitting, Electrodialysis with bipolar membranes, EDBM, Brine management, Disc reverse osmosis, DRO, Bipolar membranes, Ion exchange, EDBM plant control.

TABLE OF CONTENTS

ACKNOWLEDGEMENTS ..... **I**

ABSTRACT ..... **II**

LIST OF ABBREVIATIONS ..... **IX**

NOMENCLATURE ..... **X**

CHAPTER 1: INTRODUCTION **1**

1.1 Background and motivation **2**

1.1.1 Water and mining in South Africa 2

1.1.2 Platinum group metals and base metal refineries 2

1.1.3 Salt splitting by electrodialysis with bipolar membranes 3

1.2 Research problem **4**

1.3 Aim **4**

1.4 Objectives **4**

1.5 Investigation outline **4**

CHAPTER 2: LITERATURE STUDY **7**

2.1 Production of sodium sulphate in base metal refineries **8**

2.2 Wastewater beneficiation **9**

2.2.1 Evaporative crystallisation 10

2.2.2 Reverse osmosis 11

2.2.3 Electrodialysis 11

2.2.4 Electrodialysis with bipolar membranes 13

2.2.4.1 Bipolar membranes 13

2.2.4.2 Salt splitting by electrodialysis with bipolar membranes 15

2.3 Ion-exchange membranes 18

2.3.1 Electrochemical properties 19

2.3.2 Mass transfer 21

2.4 Economic considerations for electrodialysis with bipolar membranes 22

2.4.1 Important parameters 22

CHAPTER 3: EXPERIMENTAL METHOD 24

3.1 Experimental setup 25

3.2 Materials 27

3.3 Equipment 27

3.4 Experimental procedure 30

3.4.1 Phase 1 31

3.4.1.1 Control strategy for the saltwater tank 32

3.4.2 Phase 2 33

3.4.2.1 New control strategy for the saltwater tank 34

3.5 Analytical methods 35

CHAPTER 4: RESULTS AND DISCUSSION 36

4.1 Process control 37

4.1.1 Temperature control 37

4.1.2 Electrical conductivity control 38

4.2 Permeate flow rate tests 39

4.3 Effect of salt concentration 41

4.4 Effect of temperature 43

4.5 Circulation flowrate dependence 45

4.6 Current- and power density dependence 46

4.7 Cost estimation for the production of NaOH 47

4.8 Product compositions and purities 49

CHAPTER 5: CONCLUSIONS AND RECOMMENDATIONS 50

5.1 Conclusions 51

5.2 Recommendations 52

BIBLIOGRAPHY 54

APPENDIX A: DENSITY CALCULATIONS 59

APPENDIX B: IMPURITY CALCULATIONS 60

LIST OF TABLES

Table 3-1: Chemicals used during experiments 27

Table 3-2: Standard operating conditions for phase 1 31

Table 3-3: Experimental parameters for phase 1 32

Table 3-4: Experimental parameters for permeate flow rate tests 33

Table 3-5: Experimental parameters for phase 2 34

Table 4-1: EC vs. concentration for sodium sulphate solutions at 35°C 43

Table 4-2: Effect of temperature on EDBM performance 44

Table 4-3: Effect of electrolyte flow rate on EDBM performance 46

Table 4-4: Equipment cost and EDBM cost factors 48

Table 4-5: Average product compositions and impurities for the 91 mS/cm and 121 mS/cm case. 49

LIST OF FIGURES

Figure 1-1: Block flow diagram of small scale EDBM-DRO plant 5

Figure 2-1: Matte-smelting-refining process to recover PGMs from ore (Panda et al., 2018)..... 8

Figure 2-2: Simplified schematic of a BMR (Hagemann & Pelser, 2016). 9

Figure 2-3: Diagram of a multi-effect evaporative crystalliser (Fernández-Torres *et al.*, 2012)..... 10

Figure 2-4: A schematic diagram of RO..... 11

Figure 2-5: Principle of the concentration process by electrodialysis (Kemperman, 2000). 12

Figure 2-6: Water splitting in a bipolar membrane (Kemperman, 2000). 14

Figure 2-7: Electrodialysis with bipolar membranes for the conversion of a salt (MX) into its respective acid (HX) and base (MOH) (Kemperman, 2000). 16

Figure 2-8: Various processes occurring in the EDBM stack (Kemperman, 2000). 17

Figure 2-9: Structure of a cation-exchange membrane (Strathmann, 2004)..... 18

Figure 3-1: P&ID of the small scale sodium sulphate salt splitting plant used to conduct experiments. 25

Figure 3-2: Schematic of the EDMB module (FUMATECH, 2020). 28

Figure 3-3: Schematic of the DRO module (Newater technology, 2021)..... 29

Figure 3-4: Schematic of the control strategy for the saltwater tank during phase 1 32

Figure 3-5: Schematic of the control strategy for the saltwater tank during phase 2 35

Figure 4-1: Temperatures in the saltwater, acid and caustic tanks throughout a 40-minute experiment. 37

Figure 4-2: Electrical conductivity in the saltwater, acid and caustic tanks. 38

Figure 4-3: Setpoint tracking in the saltwater tank together with the corresponding mass change in the saltwater feed tank. 39

Figure 4-4: Permeate flow rate vs pressure for four cases 40

Figure 4-5: pH of permeate vs pressure 41

Figure 4-6: EC vs concentration at 35 °C 42

Figure 4-7: SSR (a), CPR and SEC (b) and APR (c) vs overall electrical conductivity 42

Figure 4-8: Effect of temperature on EC 44

Figure 4-9: Schematic of concentration polarisation at the feed side (Luis, 2018) 45

Figure 4-10: Specific rates vs current density for 91 mS/cm (a) and 121 mS/cm (b) 46

Figure 4-11: SEC_{NaOH} vs power density 47

Figure 4-12: Sodium hydroxide production cost vs power density 48

LIST OF ABBREVIATIONS

Abbreviation	Meaning
ACE	Associated Chemical Enterprises
AEM	Anion exchange membrane
APR	Acid production rate
BMR	Base metal refinery
BPM	Bipolar membrane
CEM	Cation exchange membrane
CPR	Caustic production rate
DC	Direct current
DRO	Disk reverse osmosis
EC	Electrical conductivity
ED	Electrodialysis
EDBM	Electrodialysis with bipolar membranes
GDP	Gross domestic product
ICP-OES	Inductively coupled plasma – Optical emission spectroscopy
IEM	Ion exchange membrane
MIMO	Multiple-input-multiple-output
P&ID	Piping and instrumentation diagram
PGM	Platinum group metal
PVDF	Polyvinylidene Difluoride
RO	Reverse osmosis
SEC	Specific energy consumption
SFR	Salt feed rate
SP	Setpoint
SSR	Salt splitting rate
ZLD	Zero liquid discharge

NOMENCLATURE

Symbol	Representation	Unit/Value
a	Activity of chemical species	-
A	Area	m^2
$\mu°$	Chemical potential in standard state	J/mol
C	Concentration	mol/L
k	Conductivity	S/m
v_k	Convective flow	m/s
I	Current	A
j	Current density	A/m^2
ξ	Current efficiency	-
D	Diffusion coefficient	m^2/s
L	Distance	m
E_{Don}	Donnan potential	V
Ω	Electrical resistance	Ω
n	Electrochemical potential	J/mol
F	Faraday constant	96 485 A·s/mol
J	Flux	$mol/m^2/s$
R	Gas law constant	8.1345 J/mol/K
r	Gibbs-Donnan ratio	-
u	Ion mobility	m^2·mol/J/s
z	Ion valence	-
K	Kohlrausch coefficient	$mS·L^{3/2}/cm/mol^{3/2}$
M	Mass transfer	mol/s
Λ_m	Molar conductivity	mS·L/cm/mol
$\Lambda°_m$	Molar conductivity at infinite dilution	mS·L/cm/mol
n^*	Molar flux density	$mol/m^2/s$
Mw	Molecular weight	g/mol
π	Osmotic pressure	Pa
V	Potential difference	V
v	Stoichiometric coefficient	-
T	Temperature	K
E	Thermodynamic component of the electrode potential	V
ΔE	Total potential drop	V

i	Van’t Hoff’s factor	-

CHAPTER 1: INTRODUCTION

Chapter 1 provides a background on the impact of mining on the quality of water in South Africa with emphasis on the production of brine in base metal refineries. Current methods of treating wastewater are mentioned, and an alternative is proposed. Sections 1.2, 1.3 and 1.4 discusses the research problem, aim and objectives, respectively. The chapter is closed in section 1.5, outlining the scope of the study.

1.1 Background and motivation

1.1.1 Water and mining in South Africa

Water is considered the most fundamental and indispensable natural resource. Environmental diversity, social- and economic development cannot be sustained without water. Worldwide, countries are struggling to meet the growing demand for water driven by industrialization, mechanization and urbanization (Ochieng *et al.*, 2010). South Africa has an annual rainfall of 500 mm, which is lower than the global average of 860 mm. This low rainfall and variability in rainfall across wet eastern and dry western regions pose a great challenge to water security in South Africa (Sinha & Kumar, 2019). It is thus of utmost importance to reduce salinization by industries in South Africa.

Mining plays an important role in the South African economy, being responsible for 7.5% of the country's gross domestic product (GDP) in 2017 (Department of mineral resources, 2017). South Africa has the largest reserves of gold, platinum, titanium, chromium, manganese and vanadium in the world (Stilwell *et al.*, 2000). The mining industry only utilizes 3% of the country's water but this has a deteriorating effect on the water quality due to pollution (Haggard *et al.*, 2015). The process water should thus be treated to minimise the negative effect that it has on the environment.

1.1.2 Platinum group metals and base metal refineries

Platinum (Pt), palladium (Pd), rhodium (Rh), ruthenium (Ru), iridium (Ir) and osmium (Os) are called platinum group metals (PGMs) and are mostly used as catalysts to minimize emissions from vehicles (Crundwell *et al.*, 2011). It is estimated that 80% of platinum group metal deposits are located in South Africa (Africa mining iQ, 2021), therefore platinum group metal mining is an important part of South Africa's mining sector. The production of base metals such as copper and nickel are coupled with platinum group metal production.

The base metals, copper and nickel, are leached from a platinum group metal rich matte using sulphuric acid as a lixiviant forming a copper and nickel rich solution as well as a platinum group metal rich concentrate. Electrowinning tanks are used to obtain nickel and copper metal from the solution. The spent electrolyte from the nickel tank is neutralised by adding sodium hydroxide to precipitate the remaining nickel (Hagemann & Pelser, 2016). A sodium sulphate solution is formed (Hagemann & Pelser, 2016) which cannot be discarded due to its high salinity (HERA, 2006).

Currently, water is evaporated from the sodium sulphate solution to form sodium sulphate crystals in a process called evaporative crystallisation (Hagemann & Pelser, 2016). Evaporative crystallisation is an energy-intensive process and in this case, it produces a salt with low value (Lu *et al.*, 2017). A proposed alternative to evaporative crystallisation is salt splitting by electrodialysis with bipolar membranes (EDBM) integrated with disk reverse osmosis (DRO). Using electrodialysis with bipolar membranes integrated with disk reverse osmosis to treat a sodium sulphate solution will produce process water, sodium hydroxide and sulphuric acid that each can be recycled to the base metal refinery (BMR).

1.1.3 Salt splitting by electrodialysis with bipolar membranes

Electrodialysis (ED) is the most common electro-membrane process and is used for the desalination and concentration of aqueous solutions. Ions move in the direction of the oppositely charged electrode under the influence of an applied direct-current field. An anion-exchange membrane blocks the cations and a cation-exchange membrane retains the anions, resulting in a concentration of the ions on one side of the membrane and a dilution of the ions on the other side of the membrane. The term, cell pair, refers to a combination of an anion-exchange membrane, a cation-exchange membrane, a concentrate chamber, and a dilute chamber. A multitude of cell pairs can be arranged between one pair of electrodes (Kemperman, 2000).

The invention of bipolar membranes (BPMs) has greatly extended the potential of electrodialysis. Bipolar membranes supply H^+ and OH^- ions without producing H_2 and O_2 as by-products (except at the outer electrodes of the stack), giving it an energetic advantage over conventional electrolytic water splitting. This major advantage allows for different extensions of electrodialysis (Kemperman, 2000).

Van der Westhuizen (2019) showed that salt splitting by electrodialysis with bipolar membranes is an economically viable solution for the treatment of base metal refinery wastewater by splitting the sodium sulphate solution into sulphuric acid and sodium hydroxide. The study showed that it is more economical to operate the process at high salt concentrations and high temperature. The temperature of the sodium sulphate solution is, however, limited by the maximum operating temperature of the membranes. The salt concentration can be increased by concentrating the sodium sulphate solution using disk reverse osmosis.

1.2 Research problem

Currently, sodium sulphate is recovered from salt solutions through expensive evaporative crystallisation, resulting in a salt with low to zero value. Using electrodialysis with bipolar membranes integrated with disk reverse osmosis to treat the sodium sulphate solution will produce process water, sodium hydroxide and sulphuric acid that can be recycled to the base metal refinery, making it a promising alternative to evaporative crystallisation. Van der Westhuizen (2019) showed in batch experiments that salt splitting by electrodialysis with bipolar membranes is an economically viable alternative to evaporative crystallisation, but the knowledge gap between batch tests and the demonstration plant at the mining site has not yet been bridged.

1.3 Aim

The study aims to design a continuous EDBM - DRO process with a robust control system and to minimise the production cost of sodium hydroxide via manipulation of the salt concentration, temperature, and current density.

1.4 Objectives

- Show that the continuous electrodialysis with bipolar membranes integrated with disk reverse osmosis process is technically viable.
- Design and implement a control system.
- Optimise sodium hydroxide production cost via salt concentration, temperature, and current density.

1.5 Investigation outline

An in-depth literature study will outline the study and will contain sources on current wastewater beneficiation techniques, the workings of ion-exchange membranes and the economic considerations for electrodialysis with bipolar membranes.

The experimental method will follow, in which data on the effects of different parameters on the production rates of sodium hydroxide and sulphuric acid will be produced. The control strategy will also be described.

A block flow diagram of the small scale plant that will be used is shown in Figure 1-1. Stream 1 is the feed to the salt tank while stream 2 is the saltwater feed to the EDBM module. Streams 3 and 4 represent the sodium hydroxide and sulphuric acid streams from the EDBM module respectively. Stream 5 is the sodium hydroxide product stream and stream 6 is the sulphuric acid product stream with concentrations of 60 g/L and 40 g/L respectively. Stream 7 is the saltwater feed to the DRO module and stream 8 is the permeate from the DRO module. Streams 9 and 10 are used to dilute the caustic and acid tanks respectively to prevent damage to the membranes of the EDBM module.

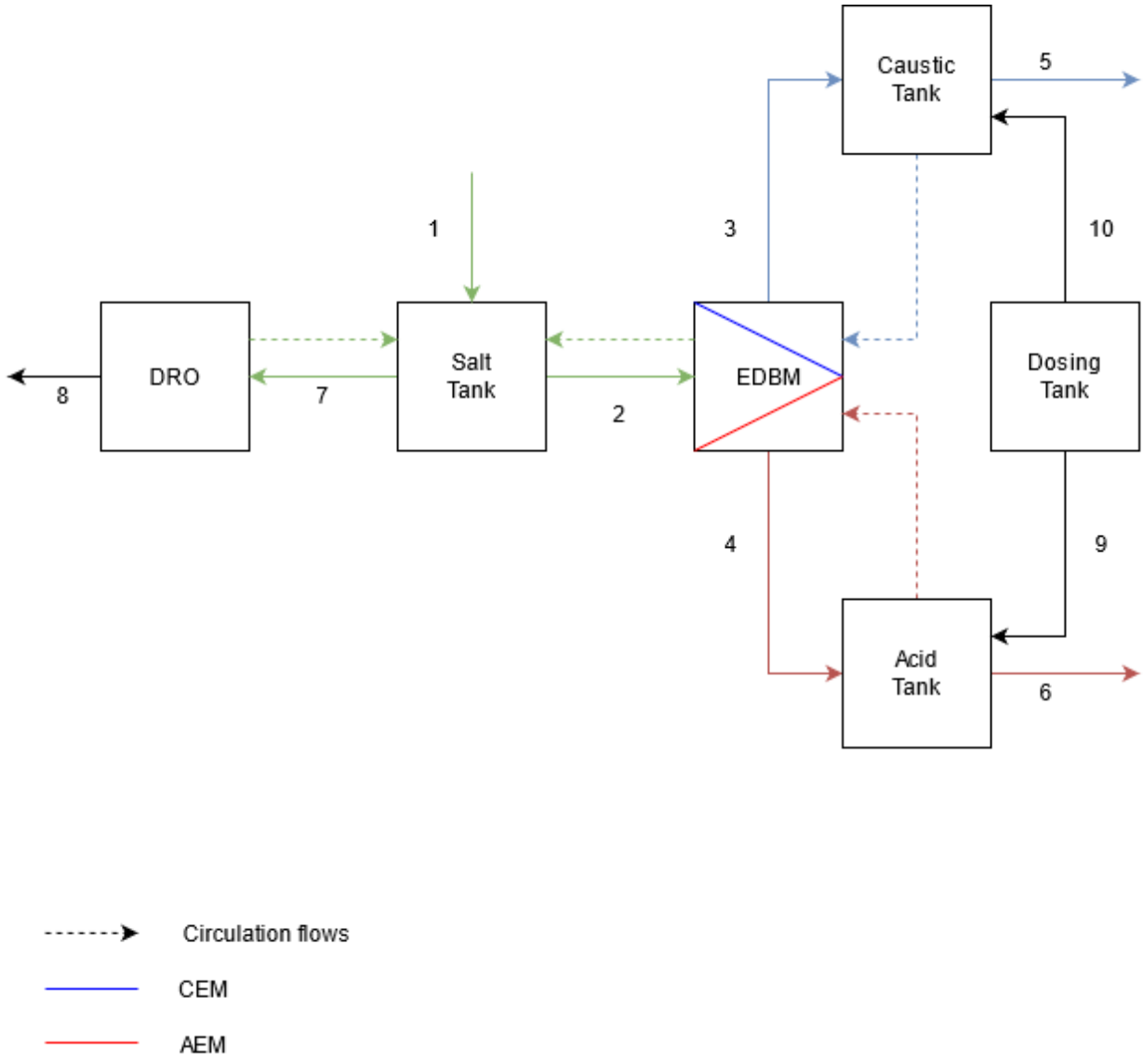

Figure 1-1: Block flow diagram of small scale EDBM-DRO plant

The experimental data will be used to evaluate the efficiency of the control method and the effects of different parameters on the production rates. The report will end with a conclusion chapter as the final chapter.

CHAPTER 2: LITERATURE STUDY

Chapter 1 explained the background and motivation behind the study and it outlined the research problem, aim and objectives of the study. It was concluded by an investigation outline, explaining the method and scope of the study. Chapter 2 investigates literature with regards to base metal refineries and methods for wastewater beneficiation. This is followed by a detailed section on ion-exchange membranes and salt splitting by electrodialysis with bipolar membranes before explaining the economic considerations that should be taken into account for processes utilising electrodialysis with bipolar membranes.

2.1 Production of sodium sulphate in base metal refineries

PGM ores can be classified as PGM dominant or Ni-Cu dominant. PGM dominant ores are exploited for their PGMs with other elements such as copper (Cu), nickel (Ni) and cobalt (Co) being produced as co-products. Co-products in these ores are usually of little economic value compared to PGMs. Ni-Cu dominant ores are exploited mainly for their Ni and Cu content with the PGMs produced as a co-product. In these ores, the economic value of the PGM content can range from minor to a deciding factor on the viability of the project (Cole & Ferron, 2002).

A matte-smelting-refining process is used to recover PGMs from high-grade ores as seen in Figure 2-1 (Panda *et al.*, 2018).

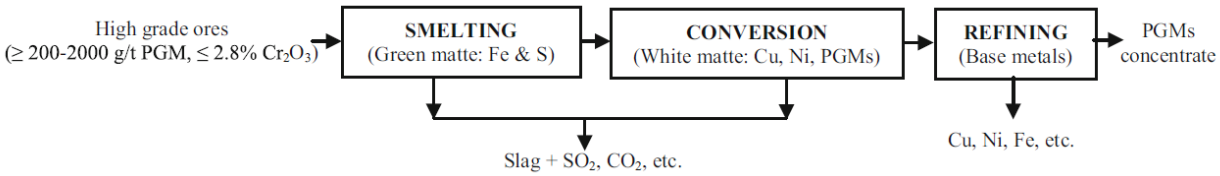

Figure 2-1: Matte-smelting-refining process to recover PGMs from ore (Panda et al., 2018).

The ore is ground before smelting and a material called matte is formed. Impurities are removed from the matte before it is cooled and sent to a base metal refinery as seen in Figure 2-2 (Panda *et al.*, 2018). The matte is milled and magnetically separated to form a non-magnetic Cu and Ni-rich matte and a magnetic PGM rich matte. The remaining Cu and Ni is leached from the PGM rich matte using sulphuric acid. Further leaching and purification steps separate Cu from Ni and sulphides are oxidised to form soluble sulphates. Electrowinning is used to obtain Cu and Ni from their corresponding electrolytes. Sulphate is removed from the spent Ni-electrolyte in the sulphur removal section. Sodium hydroxide is added to the spent nickel electrolyte to precipitate the nickel ions as nickel hydroxide, whereafter it is filtered and returned to the process. Water is evaporated from the sodium sulphate solution to obtain sodium sulphate crystals and recovered as condensate. The sodium sulphate crystals are sold but have low economic value (Hagemann & Pelser, 2016).

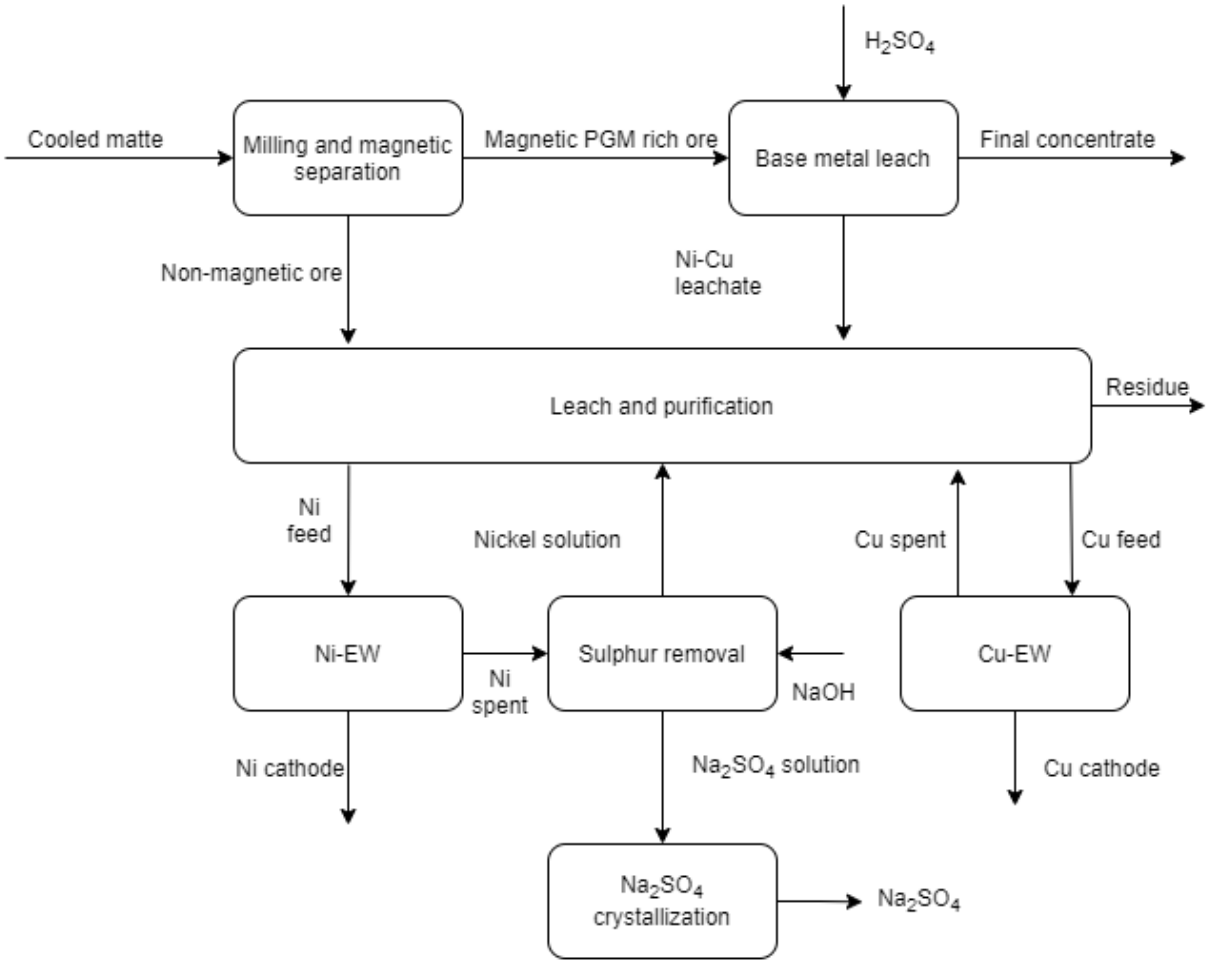

Figure 2-2: Simplified schematic of a BMR (Hagemann & Pelser, 2016).

2.2 Wastewater beneficiation

The sodium sulphate solution that is formed by the process described in section 2.1 generally has a concentration of around 100 g Na_2SO_4/L (Hagemann & Pelser, 2016). Discharging solutions with such high concentrations into the environment can upset the biodiversity of nearby water sources due to its high salinity (HERA, 2006). Hence, viable and cost-effective brine management systems are needed to prevent and reduce pollution (Panagopoulos *et al.*, 2019). Section 2.2 will discuss various zero liquid discharge (ZLD) methods of waste stream beneficiation. ZLD technologies aim to discharge no liquid effluent into surface water (El Cham *et al.*, 2020). Currently, the most widely used method is evaporative crystallisation (Lu *et al.*, 2017).

2.2.1 Evaporative crystallisation

Evaporative crystallisation is the process of crystallising a solute from a solvent by adding heat to the system. The solvent is evaporated from the unsaturated solution by an external heat source. The solution will reach saturation and any further evaporation of the solvent will result in the crystallisation of the solute from the saturated solution. Multi-effect evaporation crystallisation is the most widely used evaporative crystallisation technique due to its maturity and efficiency (Lu *et al.*, 2017). A detailed flowsheet diagram of a multi-effect evaporative crystalliser is shown in Figure 2-3. A feed stream of sodium sulphate solution is mixed with a recycled stream of saturated sodium sulphate solution. The first evaporator is heated by a closed circuit of steam and water. Some solvent evaporates to form vapour stream 1 and the rest of the solution forms liquid stream 1, a more concentrated solution. Vapour stream 1 is used to heat the second evaporator and the process is repeated. Finally, 3 phases exit the crystalliser, steam (vapour 3), anhydrous sodium sulphate (sodium sulphate crystals) and saturated solution. The saturated solution is recycled and mixed with the feed stream and the steam is condensed to form the necessary vacuum.

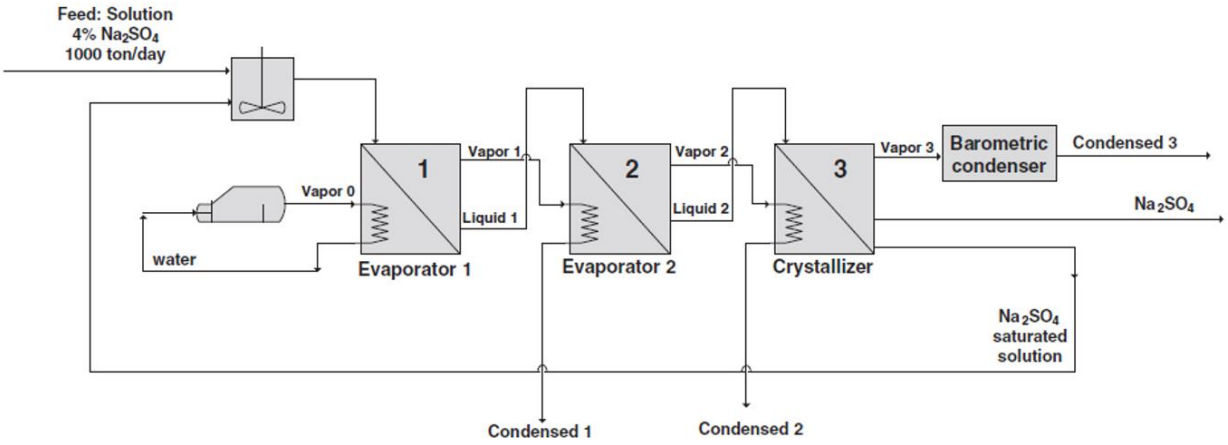

Figure 2-3: Diagram of a multi-effect evaporative crystalliser (Fernández-Torres *et al.*, 2012).

Evaporative crystallisation produces clean water that can be discarded into the environment or used as process water and sodium sulphate crystals that can be sold. The main disadvantages of evaporative crystallisation are the large capital cost, high energy consumption and the production of salt with a low economic value (Lu *et al.*, 2017).

2.2.2 Reverse osmosis

Reverse osmosis (RO) is the most commonly used membrane-based technology for desalting saline water. Reverse osmosis is based on a property of certain polymers called semi-permeability. The membranes are very permeable for water but their permeability for dissolved substances are low. A pressure difference across the membrane is needed to force water from a high salt concentration to a low salt concentration through a semi-permeable membrane as seen in Figure 2-4 (Fritzmann *et al.*, 2007).

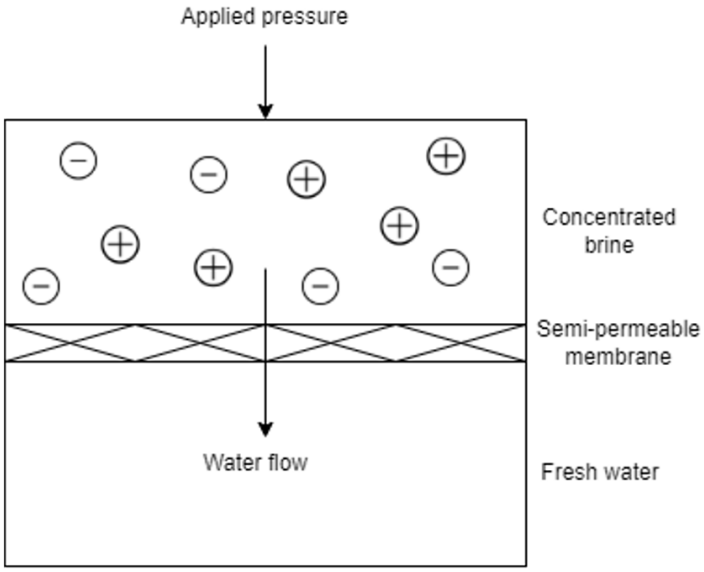

Figure 2-4: A schematic diagram of RO

The osmotic pressure of a saline solution is directly proportional to the concentration of salt and the difference between the applied pressure and the osmotic pressure is the driving force that separates the salt and water. Conventional reverse osmosis membranes and modules can be used for pressures of up to 82 bar (Panagopoulos *et al.*, 2019), thus the osmotic pressure of 100 g Na_2SO_4 is too high for conventional reverse osmosis, therefore, ultra-high pressure modules are needed that can either be in the disc or spiral wound configuration and can be operated at pressures of 120 -140 bar (Saltworks, 2020).

2.2.3 Electrodialysis

Electrodialysis is the most common electro-membrane process and can be considered as a state-of-the-art process for the desalination and concentration of aqueous solutions (Kemperman,

2000). Figure 2-5 illustrates the workings of electrodialysis. The electrodialysis unit is referred to as a stack and can consist of a few hundred membranes. A series of anion exchange membranes (AEMs) and cation exchange membranes (CEMs) are arranged in an alternating pattern to form individual cells. A volume surrounded by two adjacent membranes is termed a cell. An applied electrical potential between the anode and cathode serves as the driving force for ion transport in electrodialysis. The electric field results in the migration of negatively charged ions (anions) towards the anode and positively charged ions (cations) towards the cathode. The anions pass through the anion exchange membranes, but are retained by the cation exchange membranes and the cations pass through the cation exchange membranes, but are retained by the anion exchange membranes. The result is an increase in ion concentration in alternate compartments and a decrease in ion concentration in the other compartments (Kemperman, 2000).

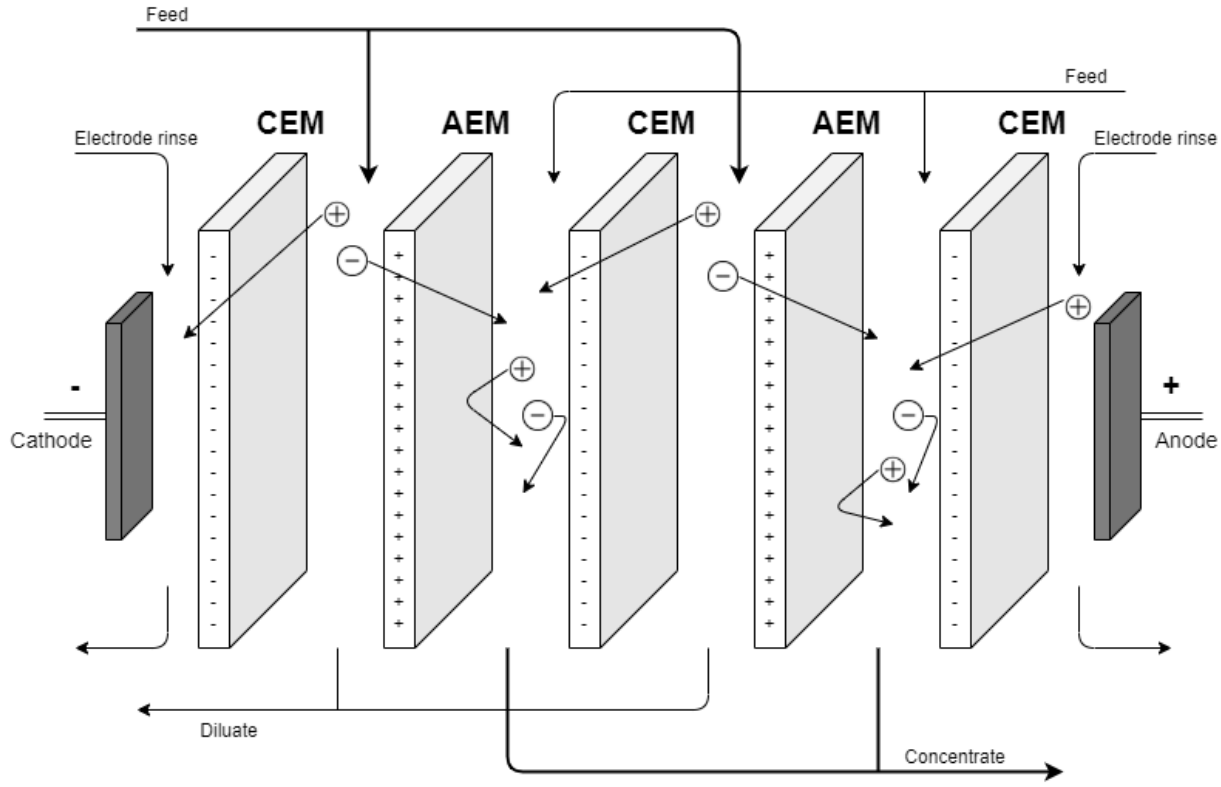

Figure 2-5: Principle of the concentration process by electrodialysis (Kemperman, 2000).

In theory, a Faraday passing through a pair of membranes is capable of carrying one equivalent gram of electrolyte from one diluted compartment to a concentrated one (Kemperman, 2000). The yield of the process can thus be multiplied “n” times by adding “n” pairs of membranes. The system resembles a set of resistors in series and the total electrical resistance includes contributions from the electrodes, membranes and the solutions that flow between the membranes. The total

electrical resistance between the two electrodes limits the number of membrane pairs that can be added to a stack. The main contribution to the electrical resistance should be associated with the produced diluted solution, meaning the membrane resistance should be as low as possible (Bernardes *et al.*, 2014). The desalination of sea and surface water to produce drinkable water or table salt is one major application of electrodialysis. The membranes used in these applications can have lifetimes of up to 17 years (Kemperman, 2000) and are subject to deterioration by fouling and scaling (Bernardes *et al.*, 2014).

2.2.4 Electrodialysis with bipolar membranes

Through the invention of bipolar membranes, the potential of electrodialysis has been greatly extended, because it restricts hydrogen and oxygen production to the electrode compartments, resulting in a considerable reduction in energy consumption (Kemperman, 2000). Electrodialysis with bipolar membranes technology integrates solvent and salt dissociation and thus inherently poses economic and environmental benefits. The development of electrodialysis with bipolar membranes technology has been restricted by factors such as the lack of recognition of its contribution to industrial ecology, high membrane cost, insufficient research investment and scarce operation experience (Huang & Xu, 2006).

2.2.4.1 Bipolar membranes

The structure and function of a bipolar membrane is illustrated in Figure 2-6. It consists of an anion- and a cation-selective layer joined together. Charged species will be removed from the transition region between the two ion-exchange layers when an electric field is established across the membrane. Transport of electric charge can only be accomplished by protons and hydroxyl ions in the absence of salt ions. Water is transported into the membrane from the surrounding areas to replenish the removed protons and hydroxyl ions (Kemperman, 2000).

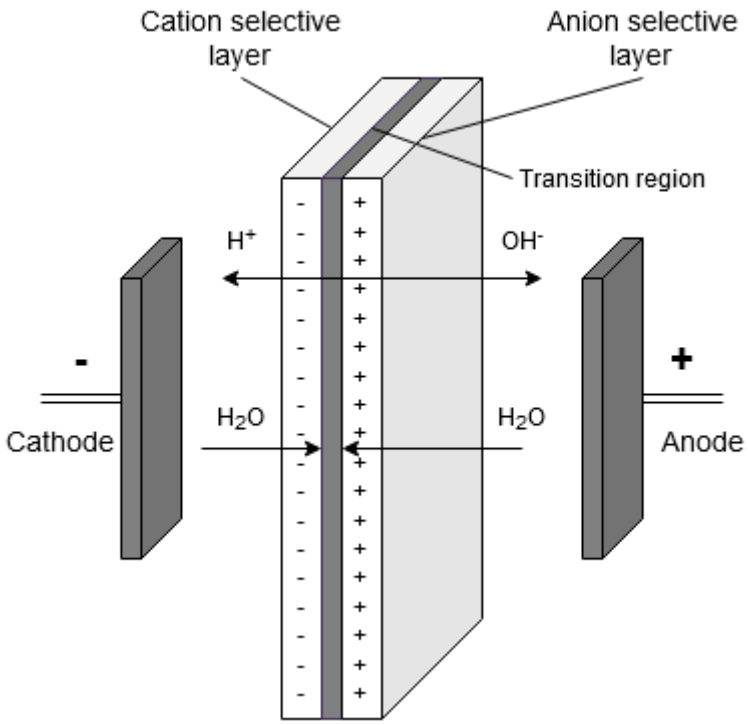

Figure 2-6: Water splitting in a bipolar membrane (Kemperman, 2000).

Water dissociation in bipolar membranes as seen in Equation (2-5), is up to 50 million times faster compared to water dissociation in aqueous solutions and is influenced by the strong electric field applied across the transition region (Kemperman, 2000). The enhanced water dissociation is due to a reversible protonation and deprotonation of the functional groups of the ion exchange membranes. The mechanism for the water dissociation reaction was proposed by Strathmann *et al.* (1997) and is given in equations 2-1 – 2-4, the overall reaction is given in equation 2-5.

$$B + H_2O \rightleftharpoons BH^+ + OH^- \quad (2\text{-}1)$$

$$BH^+ + H_2O \rightleftharpoons B + H_3O^+ \quad (2\text{-}2)$$

And

$$A^- + H_2O \rightleftharpoons AH + OH^- \quad (2\text{-}3)$$

$$AH + H_2O \rightleftharpoons A^- + H_3O^+ \quad (2\text{-}4)$$

Where B is a neutral base (AEM) and AH a neutral acid (CEM). The overall reaction is thus:

$$2H_2O \rightleftharpoons H_3O^+ + OH^- \quad (2\text{-}5)$$

The advantages of water splitting with a bipolar membrane can be summarised as follows:

- The bipolar membrane can dissociate water into H^+ and OH^- ions.
- The energy consumption is kept low since no gases are produced during water splitting.
- No oxidation and reduction reactions take place due to the absence of electrochemical reactions. This minimises the undesired reactions that may take place.
- You only need electrodes at the ends of the stack.

Salts can be converted to their corresponding acids and bases using electrodialysis when a bipolar membrane is associated with an anion exchange membrane and a cation exchange membrane. This process is called salt splitting by electrodialysis with bipolar membranes and is discussed in section 2.2.4.2.

2.2.4.2 Salt splitting by electrodialysis with bipolar membranes

The production of acid and base from saltwater using an EDMB module is shown in Figure 2-7. A salt solution (MX) is fed to the stack and under the influence of an electric field, the anions (X^-) cross the anion exchange membrane into the acid compartment and combine with protons, produced by the bipolar membrane, to form the acid (HX). The cations (M^+) cross the cation exchange membrane into the base compartment and combine with hydroxyl ions, produced by the bipolar membrane, to form the base (MOH). The anion exchange membrane, cation exchange membrane, bipolar membrane, base compartment, acid compartment and salt compartment together is termed the cell triplet. A multitude of cell triplets can be placed between one pair of electrodes (Kemperman, 2000).

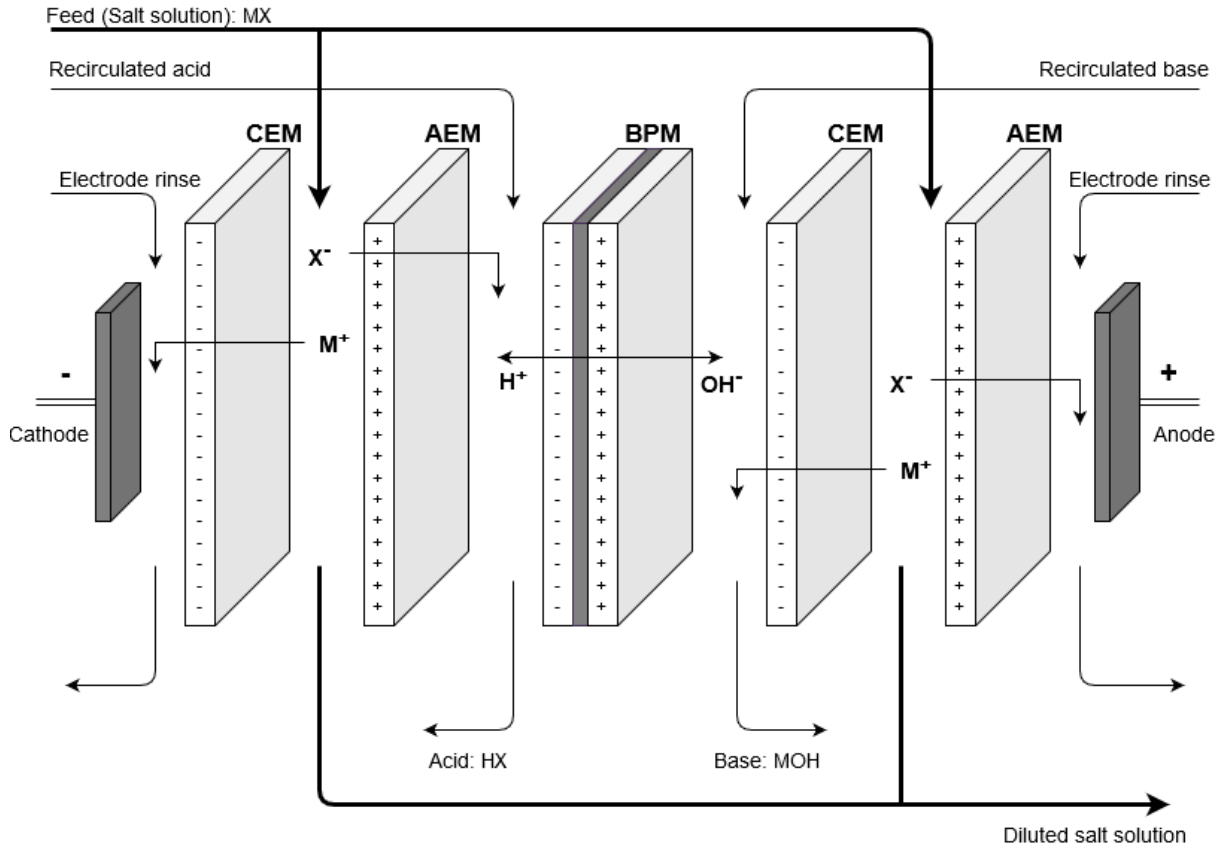

Figure 2-7: Electrodialysis with bipolar membranes for the conversion of a salt (MX) into its respective acid (HX) and base (MOH) (Kemperman, 2000).

The general overall reaction is thus:

$$MX + H_2O \rightarrow HX + MOH \quad (2\text{-}6)$$

And in the case of sodium sulphate, the reaction is:

$$Na_2SO_4 + 2H_2O \rightarrow H_2SO_4 + 2NaOH \quad (2\text{-}7)$$

Producing acids and bases with high concentrations using only electrodialysis with bipolar membranes is neither practical nor economical. Firstly, water electro-osmosis and product diffusion limit product concentration. Secondly, increasing the concentration of electrolytes (including salts, acids and bases) decreases the permselectivity of bipolar membranes and thus lowers the product purity due to co-ion migration. Thirdly, the lifetime of membranes is decreased in high concentration acids and bases. And finally, some products will crystallise, precipitate or volatilise when their concentrations exceed their solubility (Huang & Xu, 2006). Figure 2-8

illustrates the various processes which contribute to the overall current efficiency. The current efficiency is the ratio of moles produced product from an electrolyte to the maximum theoretical product that can be produced (Davis *et al.*, 2008). It is thus an indication of the amount of electric current converted to the desired product and should be kept high (Kemperman, 2000). Zone 1 represents the desired process which converts salt and water into acid and base. Zone 2 is a representation of the loss in permselectivity of each homopolar layer of the bipolar membrane. Zone 3 represents the loss of permselectivity of the anion exchange membrane and cation exchange membrane respectively and zone 4 is concerned with the diffusional losses due to concentration gradients (Mani, 1991). Therefore, the highest concentration remains to be optimized for different operation requirements (Huang & Xu, 2006).

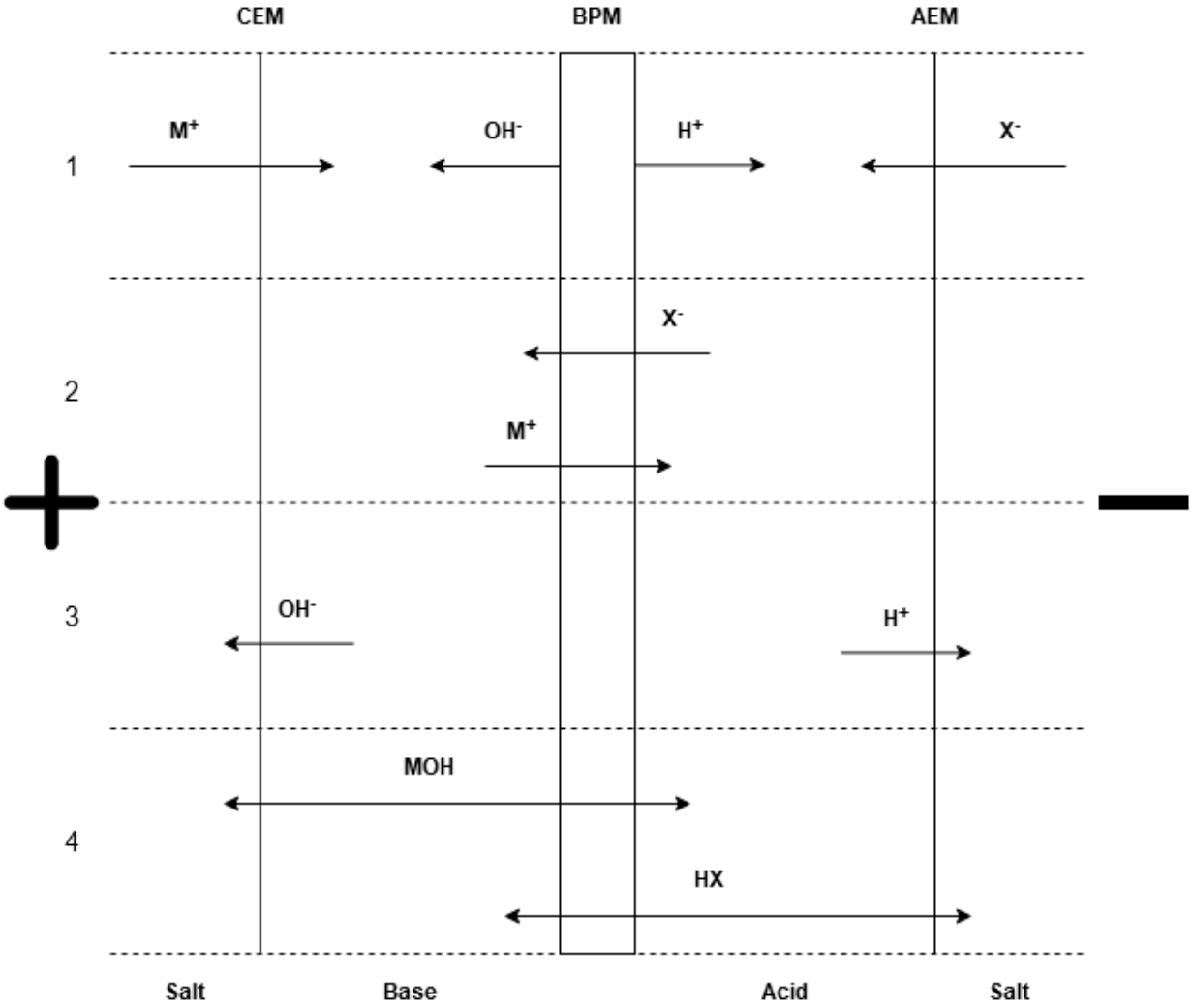

Figure 2-8: Various processes occurring in the EDBM stack (Kemperman, 2000).

The chemical stability and the resistance to fouling of the membranes play an important role in the long term operation of the EDBM process. The feed stream often needs to be treated as the bipolar membranes can be damaged by multivalent ions and organic compounds, increasing the overall cost of the process (Tongwen, 2002). Also, the product concentrations and purities need to be high enough for it to be recycled to the base metal refinery.

2.3 Ion-exchange membranes

An ion-exchange membrane (IEM) is a semi-permeable membrane that transports only certain dissolved ions, depending on their charge, while blocking other ions and neutral molecules (Tanaka, 2015). The ion exchange membrane is the most important part of any electro-membrane process and usually consists of a polymer film with ionic groups attached to the polymer backbone as shown in Figure 2-9. The fixed charges of the ionic groups can be anionic or cationic. Anions move freely through the cationic fixed charges and cations move freely through the anionic fixed charges. The moveable ions are called counter-ions as it balances the charge of the fixed ions (Kemperman, 2000). Co-ions are mobile ions in the interstices of the polymer matrix, excluded from the polymer matrix because of their identical charge to that of the fixed ions.

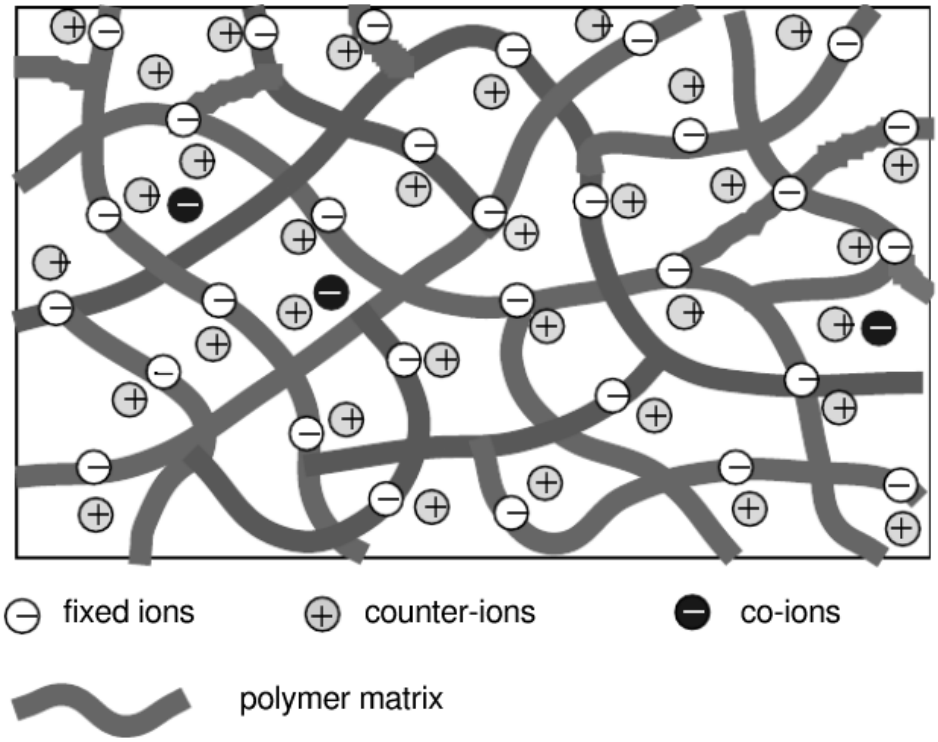

Figure 2-9: Structure of a cation-exchange membrane (Strathmann, 2004).

ion exchange membranes need to have (Eisenberg & Yeager, 1984):

- Chemical, mechanical and thermal stability
- High permselectivity
- Low electrical resistance

2.3.1 Electrochemical properties

Ohm's law is used to describe the relationship between the electrical current, voltage and electrical resistance as seen in Equation (2-8) (Strathmann, 2004).

$$V = I \cdot \Omega \tag{2-8}$$

Where V is the potential difference (V), I is the current (A) and Ω is the resistance (Ω). The resistance of a membrane or electrolyte solution can be expressed in terms of conductivity, conducting area and the distance between electron sources as seen in Equation (2-9) (Strathmann, 2004).

$$\Omega = \frac{L}{A \cdot k} \tag{2-9}$$

With L the distance between electron sources (m), A the conducting area (m^2) and k the conductivity (S/m). The conductivity of the electrolyte solutions are dependent on the concentration according to Equation (2-10) (Horvath, 1984).

$$k = \sum_i u_i \cdot z_i \cdot v_i \cdot F \cdot C \tag{2-10}$$

The index i indicates the different ions in the solution, u_i is the ion mobility (m^2·mol/J/s), z_i is the ion valence, v_i is the stoichiometric coefficient of the ion, F is the Faraday constant (96 485 A·s/mol) and C is the concentration (mol/L).

Thermodynamics dictates that two neighbouring phases are in equilibrium only when the Gibbs free energy of both phases are equal. When the chemical species are ionic (as it is in electrolyte

solutions) the electrochemical potential, n_i, is used to describe the equilibrium according to Equation (2-11) (Davis, 2000).

$$n_i = \mu^{\circ}_i + R \cdot T \cdot lna_i + z_i \cdot F \cdot V \tag{2-11}$$

$\mu°_i$ is the chemical potential of species i in the standard state, R is the gas law constant, T is the absolute temperature, a_i is the activity of the chemical species i, z_i is the ion valence, F is the Faraday constant and V is the electric potential. There exists an equilibrium between the two liquid phases when it is in equilibrium with the membrane, and the electrochemical potential can thus be equated as seen in Equations (2-12) and (2-13) (Davis, 2000).

$$n_{i1} = n_{i2} \tag{2-12}$$

$$R \cdot T \cdot lna_{i1} + z_i \cdot F \cdot V_1 = R \cdot T \cdot lna_{i2} + z_i \cdot F \cdot V_2 \tag{2-13}$$

The same standard state exists for both liquid phases, resulting in the cancellation of the $\mu°_i$ terms. Equation (2-13) can be rearranged to find the Donnan potential as seen in Equation (2-14). The Donnan potential, E_{Don}, is the potential difference across the membrane caused by a concentration difference between the two liquid phases.

$$E_{Don} = V_2 - V_1 = \frac{R \cdot T}{F} \cdot \ln(\frac{a_{i1}}{a_{i2}})^{\frac{1}{z_i}} \tag{2-14}$$

The value for the term $(\frac{a_{i1}}{a_{i2}})^{\frac{1}{z_i}}$ is the same for all counterions in the system since the Donnan potential acts on all mobile ionic species. This means that an electrical potential that acts on the counterions is caused by a concentration difference of the co-ions. The Donnan equilibrium implies that the ionic product of the salt on either side of the ion exchange membrane will be equal according to Equation (2-15) (Donnan, 1924).

$$C_{Na,1}C_{A,1} = C_{Na,2}C_{A,2} \tag{2-15}$$

The subscript *1* and *2* denotes each side of the membrane while Na indicates a sodium ion and A indicates any anion with a valency of 1. The Gibbs-Donnan ratio, r, is written as (Donnan, 1924).

$$r = \frac{C_{Na,1}}{C_{Na,2}} = \frac{C_{A,2}}{C_{A,1}} \tag{2-16}$$

The selectivity of an ion exchange membrane can be represented by the Donnan equilibrium and is dependent on the electrolyte concentration, valence of the ions, affinity of the ion exchange membrane to certain ions in the electrolyte and the concentration of fixed ions in the ion exchange membrane (Strathmann, 2004).

2.3.2 Mass transfer

The driving force for mass transfer in electrodialysis can be expressed by the gradients in the electrochemical potential of individual components in the solution. The mass transfer is simultaneously being resisted by friction when components move in the solution and the ion exchange membranes. The resistance that needs to be overcome by the driving force is expressed by a diffusion coefficient or by the electrical resistance of the electrolyte and membranes (Strathmann, 2004). The Nerst-Planck equation is used to describe mass transport phenomena in electrodialysis (Spiegler & Laird, 1980).

$$J_i = -D_i \cdot \frac{dC_i}{dz} - D_i \cdot \frac{z_i \cdot C_i \cdot F}{R \cdot T} \cdot \frac{V}{dz} + v_k \cdot C_i \qquad (2\text{-}17)$$

With J_i the flux (mol/m^2/s), D_i the diffusion coefficient (m^2/s), C_i the concentration (mol/m^3), z_i the ion valence, F the Faraday constant (96 485 A·s/mol), R the universal gas constant, T the absolute temperature, V the electric potential (V) and v_k the convective flow (m/s). The subscript i refers to a component and dz is a directional coordinate.
Three modes of mass transport are considered by the Nerst-Planck equation namely:

1. Diffusion due to a concentration gradient, represented by the first term in Equation (2-17).
2. Migration due to an electrical potential gradient, represented by the second term in Equation (2-17).
3. Convection due to a pressure gradient, represented by the third term in Equation (2-17).

The transport of ions in ion exchange membranes can be conveniently described by the Nerst-Planck equation (Strathmann, 2004). It is assumed that the salt in the solution is dissociated perfectly, and consequently, concentration replaces activity in the diffusion equations, relating the diffusion coefficient and mobility according to Einstein's relation as seen in Equation (2-18) (Zourmand *et al.*, 2015).

$$u_i = \frac{D_i}{R \cdot T} \tag{2-18}$$

With u_i the mobility coefficient (s·mol/kg).

2.4 Economic considerations for electrodialysis with bipolar membranes

The total process cost for electrodialysis with bipolar membranes can vary significantly depending on the location, capacity and application. The process generally aims to produce an acid and/or base or to treat industrial effluent. This means that electrodialysis with bipolar membranes competes directly with conventional processes, thus a fair cost analysis should include pre-and post-treatment procedures necessary to obtain the desired product. The required product quality, membrane properties, feed solution composition, stack construction, operating current density, etc, all have a considerable effect on the process cost and should thus be taken into account (Kemperman, 2000).

2.4.1 Important parameters

Several important performance indicators should be considered when commercialising the electrodialysis with bipolar membranes process such as the total cell voltage, current efficiency, current density and the specific energy consumption (Kemperman, 2000; Pisarska *et al.*, 2017). The total cell voltage, $I{\cdot}\Omega_{EDBMcell}$, includes the voltage drop of each elementary cell unit and the voltage drop in the electrode compartments as shown in Equation (2-19) (Kemperman, 2000).

$$I \cdot \Omega_{EDBMcell} = E_{cathode} - E_{anode} - I \cdot \Omega_{cell} - I \cdot \Omega_{circuit} = \Delta E \tag{2-19}$$

With Ω_{cell} the resistance of the electrolytes and membranes, $\Omega_{circuit}$ the resistance of the electrical connections, E_{anode} and $E_{cathode}$ the thermodynamic components of the electrode potential including the anodic and cathodic overpotentials and ΔE the total potential drop.

Each transported ionic species has a current efficiency, ξ, defined as the ratio of actual molar transport to the theoretical maximum calculated by Faraday's law (Kemperman, 2000; Tzanetakis *et al.*, 2002).

$$\xi = \frac{F \cdot z_i \cdot n^*}{j} \tag{2-20}$$

$$j = \frac{I}{A} \tag{2-21}$$

The subscript i refers to the product being formed (either sodium hydroxide or sulphuric acid). F is Faraday's constant, z is the ion valency, n^* is the molar flux density (mol/m^2/sec), j is the current density (A/m^2), I is the applied current and A is the membrane surface area (m^2). A current efficiency below 100% indicates current leaks in the cell and a membrane permselectivity of less than 100%. The energy consumption, P (W), and required membrane area, A, can be determined by Equations (2-22) and (2-23) respectively (Kemperman, 2000).

$$P = \Delta E \cdot \frac{F \cdot z_i \cdot n^*}{\xi} \cdot A \tag{2-22}$$

$$A = \frac{26801 \cdot z_i \cdot M_i}{j \cdot \xi} \tag{2-23}$$

With M_i the mass transfer (kmol/h) and the constant 26801 has units A·h/kmol. The required membrane area and the energy consumption, which in turn determines the size and cost of the equipment, is therefore determined by the current efficiency (Raucq *et al.*, 1993).

The specific energy consumption (SEC) is the amount of energy needed to split one kilogram of salt and can be determined by Equation (2-24).

$$SEC = \frac{I \cdot V}{1000 \cdot SSR} \tag{2-24}$$

With SEC in kWh/kg, the current I in Ampere, the voltage V in volts and the salt splitting rate (SSR) in kg/h. The operating costs are mainly determined by the electrical energy required and thus, to keep the operating cost low, the SEC should be kept as low as possible (Kemperman 2000).

CHAPTER 3: EXPERIMENTAL METHOD

Current methods of base metal refinery waste stream beneficiation were discussed in Chapter 2. This was followed by a detailed section on ion-exchange membranes and salt splitting by electrodialysis with bipolar membranes as well as the economic considerations with regards to electrodialysis with bipolar membrane technology. Chapter 3 outlines the laboratory equipment and materials used as well as the methods followed during the experimental phase of the investigation.

3.1 Experimental setup

Experiments were conducted on a small scale sodium sulphate salt splitting plant. The plant was designed to convert 1.5 kg Na_2SO_4/h from a sodium sulphate solution into process water, sulphuric acid and sodium hydroxide. Figure 3-1, a piping and instrumentation diagram (P&ID) of the plant, will be used to explain the process.

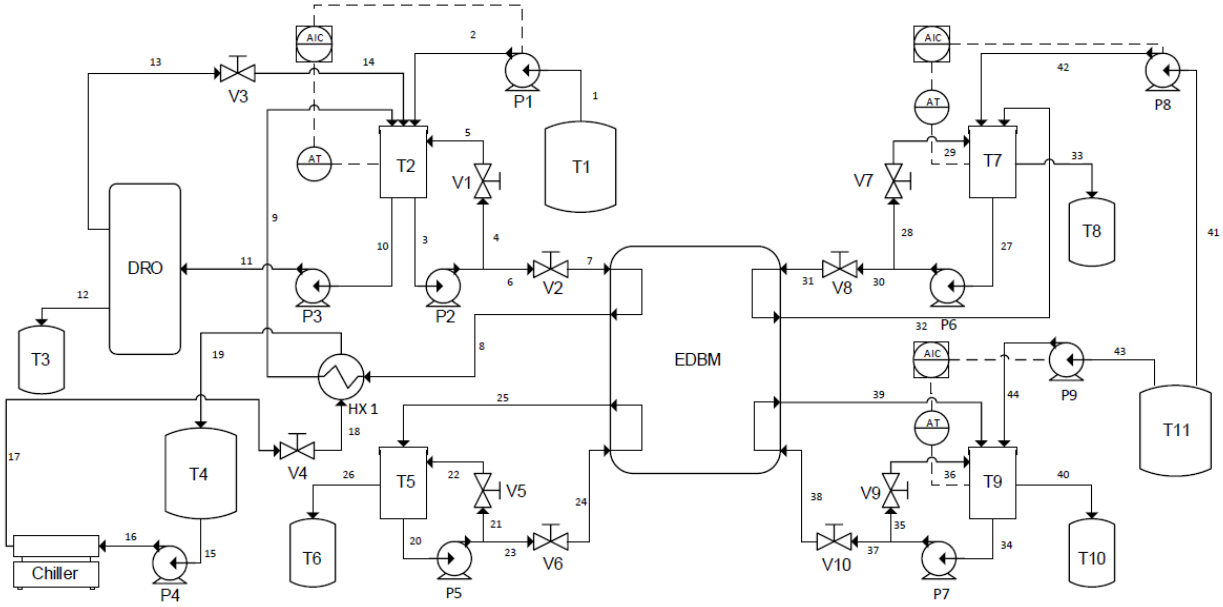

Figure 3-1: P&ID of the small scale sodium sulphate salt splitting plant used to conduct experiments.

The saltwater circuit

A sodium sulphate solution in stream 1 is fed from the saltwater feed tank (T1) using a peristaltic feed pump (P1) to the saltwater tank (T2). From here it is pumped with a centrifugal pump (P2) to two valves. A two-valve system (V1, V2) in combination with a rotameter is used to control the saltwater flow rate (7) to the EDBM module.

Stream 7 enters the EDBM module and the sodium sulphate solution is converted to sodium hydroxide and sulphuric acid as explained in section 2.2.4.2. The sodium sulphate solution leaving the EDBM module in stream 8 has a slightly lower concentration and a higher temperature than in stream 7. Stream 8 is sent through a heat exchanger (HX1) to maintain the temperature in the saltwater tank (T2) at its setpoint.

Sodium sulphate solution is pumped by a piston pump (P3) from the saltwater tank to the DRO module. Stream 11 enters the DRO module at a high pressure, regulated by valve 3 (V3). Closing valve 3 increases the retentate pressure in the DRO module and vice versa. Stream 12, the permeate from the DRO module, is collected in a water tank (T3) before it is disposed of. Stream 13, the retentate, leaves the DRO module at a high pressure and the pressure is released by valve 3 before it is returned to the saltwater tank as stream 14. The level in T2 is manually maintained at its setpoint by adjusting V3.

The cooling water circuit

Cooling water stream 15 is pumped from the cooling water tank (T4) using a submersible pump (P4) through a chiller. The cold water leaves the chiller and passes through valve 4 (V4) to the heat exchanger where it cools down the sodium sulphate solution in stream 8. Valve 4 is used to manually control the temperature in T2.

The rinse circuit

A sodium sulphate solution leaves the rinse water tank (T5) in stream 20. Sodium sulphate was added to the water to keep the conductivity high. A two-valve (V5, V6) and rotameter system is used to control the rinse water flow rate to the EDBM module. Stream 24 enters the EDBM module and removes hydrogen and oxygen produced at the cathode and anode respectively to prevent it from accumulating. Stream 25 leaves the EDBM module and is returned to the rinse water tank. If the level in the rinse water tank rises above the overflow point, it will overflow into the rinse water waste tank (T6). The temperature in the rinse circuit is maintained at its setpoint via heat transfer to the salt channels inside the EDBM module.

The caustic circuit

A two-valve (V7, V8) and rotameter system is used to control the sodium hydroxide flow rate to the EDBM module. Sodium hydroxide is produced inside the EDBM module as explained in section 2.2.4.2 and leaves the EDBM module in stream 32 at a slightly higher concentration than in stream 31. Stream 32 is recycled to the sodium hydroxide tank. Stream 33, an overflow stream from the sodium hydroxide tank, is the sodium hydroxide product stream and it flows into the sodium hydroxide product tank (T8). The electrical conductivity in the sodium hydroxide tank is maintained at its setpoint by adding dilution water from T11 via a dosing pump (P8). The temperature in the caustic circuit is maintained at its setpoint via heat transfer to the salt channels inside the EDBM module.

The acid circuit

A two-valve (V9, V10) and rotameter system is used to control the sulphuric acid flow rate to the EDBM module. Sulphuric acid is produced inside the EDBM module as explained in section 2.2.4.2 and leaves the EDBM module in stream 39 at a slightly higher concentration than in stream 38. Stream 39 is recycled to the sulphuric acid tank. Stream 40, an overflow stream from the sulphuric acid tank, is the sulphuric acid product stream and it flows into the sulphuric acid product tank (T10). The electrical conductivity in the sulphuric acid tank is maintained at its setpoint by adding dilution water from T11 via a dosing pump (P9). The temperature in the acid circuit is maintained at its setpoint via heat transfer to the salt channels inside the EDBM module.

3.2 Materials

The materials used during the experimental investigation and their specifications are summarised in Table 3-1. All chemicals were obtained from Associated Chemical Enterprises (ACE) and reverse osmosis water was obtained from Oasis in Potchefstroom. The reverse osmosis water was necessary to ensure that it did not influence the conductivity and to ensure that it could not foul the membrane.

Table 3-1: Chemicals used during experiments

Chemical	Formula	Purity
Sulphuric acid	H_2SO_4	98 %
Sodium sulphate	Na_2SO_4	99 %
Sodium hydroxide	NaOH	98 %

3.3 Equipment

Pumps

A total of 9 pumps were used during experimentation. Three dosing pumps (P1, P8, P9) were used to deliver reverse osmosis water and saltwater to their respective tanks. The dosing pumps are peristaltic pumps and have a feed rate of up to 50 L/h. Four circulation pumps (P2, P5, P6, P7) were used to pump the contents of the saltwater tank, sulphuric acid tank, sodium hydroxide tank and rinse water tank through the EDBM module at 500 L/h and 1000 L/h. A piston pump (P3) was used to pump sodium sulphate to the DRO module and a submersible pump (P4) was used to circulate the cooling water through the chiller and heat exchanger.

EDBM module

The EDBM 320-3-50 module was manufactured by FUMATECH BWT GmbH. It has 50 repeating three-compartment cells, consisting of an anion exchange membrane, cation exchange membrane and bipolar membrane. Each three-compartment cell has a salt splitting area of 320 cm^2, resulting in a total salt splitting area of 1.6 m^2. Electrodialysis with bipolar membranes combines conventional electrodialysis for salt separation with electrochemical water splitting for the conversion of a salt into its corresponding acid and base. The anion exchange membrane is developed for low proton crossover to receive a high concentration acid and the cation exchange membrane is optimised for high cation (Na^+) transport and high OH^- retention.

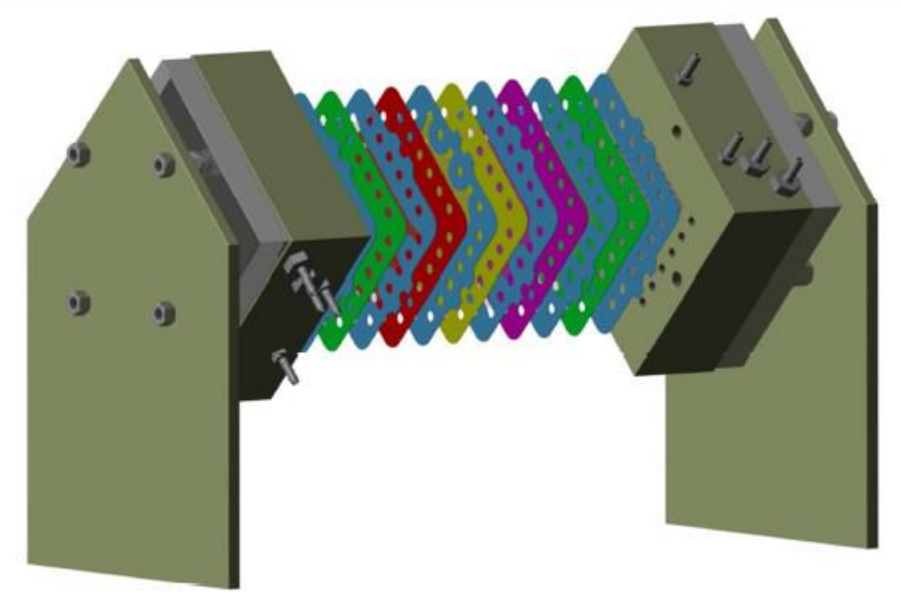

Figure 3-2: Schematic of the EDMB module (FUMATECH, 2020).

DRO module

An industrial size CD-9 DRO module with a membrane area of 9 m^2 and a maximum operating pressure of 140 bar was used to keep the concentration in the salt tank at the required setpoint.

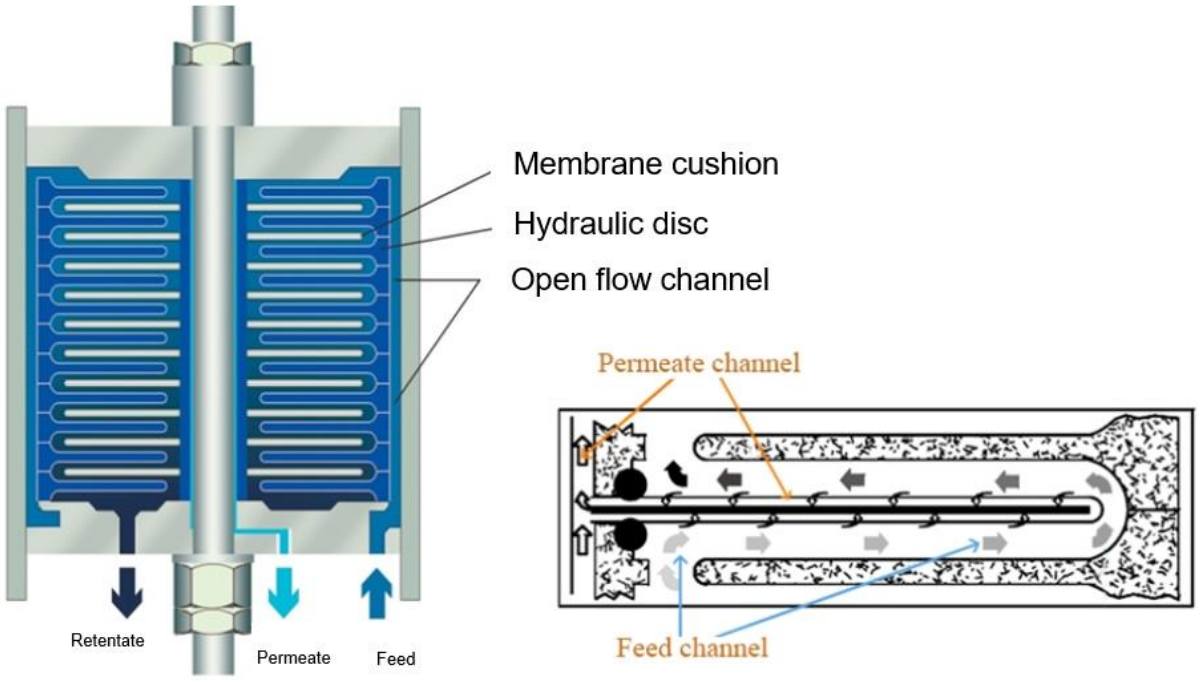

Figure 3-3: Schematic of the DRO module (Newater technology, 2021)

Power supply

The Genesys programmable direct current (DC) power supply, capable of delivering 10 kW of power, was used to power the EDBM module. It was connected to the datalogger to log the amperage and voltage data every minute.

Heat exchanger

A Calorplast polyethylene shell and tube heat exchanger was used to lower the temperature of the saltwater leaving the EDBM module. Polyethylene was used to avoid possible corrosion by the saltwater, which is detrimental for electrodialysis equipment. The heat exchanger had an effective surface area of 0.7 m^2 and an overall heat transfer coefficient of 249 $W/m^2/K$. The rate at which heat was removed from the saltwater was manually controlled by increasing or decreasing the flow rate of cooling water through the heat exchanger.

Chiller

A Teco TK3000-Aquarium chiller was used to cool down the cooling water. It sufficiently cooled the cooling water in phase 1 of the experiments, but when the piston pump (P3) was added the addition of a second chiller (Teco TK500) was needed to keep the cooling water at the desired temperature.

Pressure gauges

Rhomberg pressure gauges were connected to each membrane inlet to ensure that no blockage occurs in the respective 0.5 mm flow channels.

Flow indicators

Rotameters manufactured by Tecfluid were used to monitor the flow rates to the EDBM module. The floaters were polyvinylidene difluoride (PVDF) covered to avoid corrosion by the process streams. The flow rates were controlled by manual control valves.

Electrical conductivity (EC) and temperature sensors

The inductive conductivity sensors (Kuntze, IL 15) have an integrated temperature sensor. The sensor has a conductivity range of 0 mS/cm – 2000 mS/cm and can function under pressures of up to 10 bar at 20°C and a maximum temperature of 90°C.
These sensors are:

- Corrosion-resistant
- Dirt-resistant
- Small and robust

EC monitors

Each electrical conductivity sensor was connected to the Neon EC monitor also manufactured by Kuntze. The built-in PID functions were used to control the peristaltic dosing pumps.

Datalogger

A multi-channel data logger, the MultiLog SRD-99, manufactured by Simex was used to collect electrical conductivity and temperature data from the Neon EC monitors as well as voltage and amperage data from the power supply every minute.

3.4 Experimental procedure

The experimental plan consisted of two phases. In phase one, the concentration in the saltwater tank was controlled using an overflow system. The goal was to ensure that the equipment worked before renting the DRO module. In phase two, the DRO module was connected and the concentration in the saltwater tank was kept high by reconcentrating the saltwater. The effect of disk reverse osmosis on the control of the system was also noted.

3.4.1 Phase 1

At the start of every experiment, each tank was filled with the corresponding electrolyte at the desired concentration in order to start as close to steady-state operation as possible. The standard operating conditions are shown in Table 3-2. The conditions could then be changed to see what influence it would have on the process.

Table 3-2: Standard operating conditions for phase 1

Vessel	Concentration	Volume (L)	Temperature (°C)	Flow rate (L/h)
Saltwater tank	100 g Na_2SO_4/L	13	35	1000
Sodium hydroxide tank	60 g NaOH/L	13	37	1000
Sulphuric acid tank	40 g H_2SO_4/L	13	36	1000
Rinse water	100 g Na_2SO_4/L	13	Not measured	1000
Saltwater feed tank	150 g Na_2SO_4/L	100	Ambient	Controlled

FUMATECH recommended that the concentrations of the sodium hydroxide tank and sulphuric acid tank do not exceed 60 g/L and 40 g/L respectively. Concentrations above these values could damage the membranes of the EDBM module. The highest allowable concentrations were thus used to keep the conductivity as high as possible. The same is true for the temperature, where 40°C should be the highest temperature that the membranes should be exposed to. A setpoint temperature of 35°C for the saltwater tank was chosen. Only the temperature in the saltwater tank was controlled but the EDBM module acted as an effective heat exchanger, keeping the sodium hydroxide tank and sulphuric acid tank at 37°C and 36°C respectively. The saltwater feed tank was loaded with 150 g Na_2SO_4/L to keep the concentration in the saltwater tank constant using a P-controlled dosing pump with an overflow on the saltwater tank.

Table 3-3 shows the experimental parameters varied during phase 1 of experimentation. The salt splitting rate and specific energy consumption was used to evaluate the performance of the EDBM module. Samples from all four circulation tanks were taken throughout an experiment.

Table 3-3: Experimental parameters for phase 1

Varied Parameter	Range	Unit
Temperature (Saltwater tank)	20 – 35	°C
Circulation flow rates	500 – 1000	L/h
Applied power	500 – 3000	W
Electrical conductivity in the saltwater tank	69 – 90	mS/cm

3.4.1.1 Control strategy for the saltwater tank

The control strategy for the saltwater tank during phase 1 is shown in Figure 3-4.

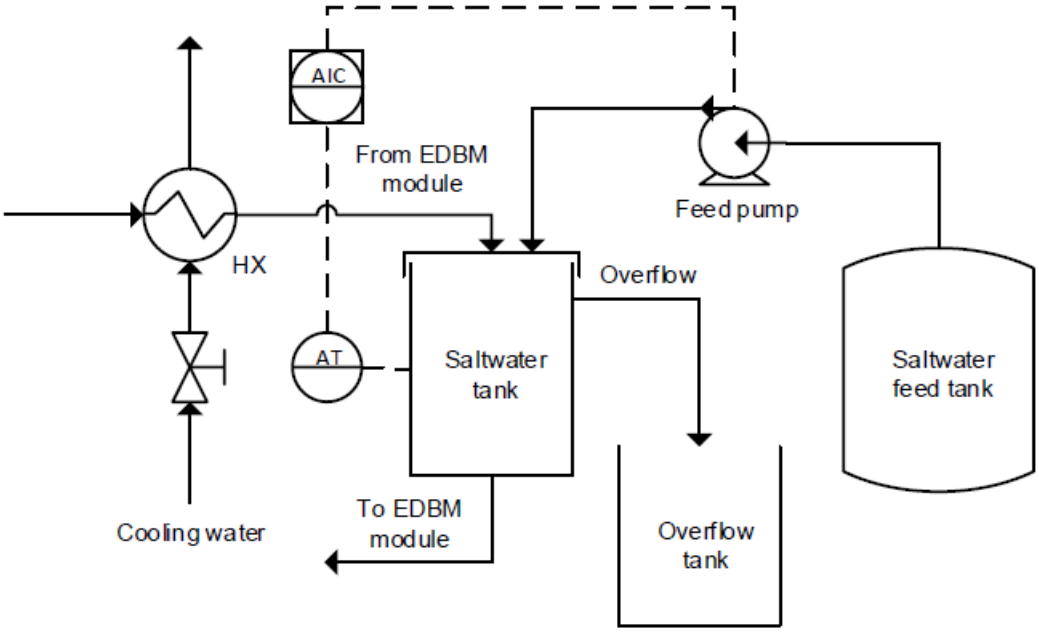

Figure 3-4: Schematic of the control strategy for the saltwater tank during phase 1

The saltwater returning to the saltwater tank from the EDBM module has a slightly lower concentration and a slightly higher temperature than the saltwater entering the EDBM module due to the salt splitting taking place. The IL 15 sensor (AT) was used to take inline measurements of conductivity and temperature and the EC monitor (AIC) was used to control the conductivity by supplying saltwater from the saltwater feed tank via the peristaltic dosing pump. P-control was used with a P-range of 1.0 mS/cm and the controller was set to increase the conductivity when it

fell below the setpoint value. The temperature in the saltwater tank was maintained at its setpoint using a heat exchanger and cooling water. The temperature was manually controlled by increasing or decreasing the flow rate of cooling water through the heat exchanger.

3.4.2 Phase 2

The DRO module replaced the overflow system in phase 1. The saltwater could now be reconcentrated instead of using an overflow to keep the concentration constant. A piston pump was used to pump water from the saltwater tank to feed the DRO module. The pressure inside the module was regulated by a valve on the retentate stream. Closing the valve will increase the backpressure and the permeate flow rate and vice versa.

A few tests were run on the disk reverse osmosis system without using the EDBM module. Table 3-4 summarises the different parameters used. The permeate flow rate from the DRO module was measured at different applied back pressures and different saltwater concentrations to determine the permeability of the membrane and to see what effect the increased salt concentration would have on the permeate flow rate at different pressures. In reality, acid would leak into the saltwater tank due to the imperfectness of the anion exchange membrane. Sulphuric acid was added to the saltwater tank and the experiments were repeated at a pH of 2 to determine what effect the lower pH would have on the permeability and permeate flow rate. The permeate and the retentate were recycled to the saltwater tank to keep the concentration constant throughout the experiment.

Table 3-4: Experimental parameters for permeate flow rate tests

Saltwater concentration (g/L)	pH	Pressure (bar)
100	7	0 – 85
150	7	0 – 85
100	2	0 – 85
150	2	0 – 85

The same standard operating conditions given in Table 3-2 applied for the experiments in phase 2, except for the concentration in the saltwater feed tank which ranged from 30 g Na_2SO_4/L to 100 g Na_2SO_4/L, depending on the experiment. The reason for this was to create a higher permeate

flow rate that better matched the oversized DRO module. The experimental parameters for phase 2 are given in Table 3-5.

Table 3-5: Experimental parameters for phase 2

Varied Parameter	Range	Unit
Circulation flow rates	500 – 1000	L/h
Applied power	1000 – 3000	W
Electrical conductivity in the saltwater tank	91 – 121	mS/cm

The salt splitting rate and specific energy consumption were used to evaluate the performance of the EDBM module. Samples from all four circulation tanks as well as from the retentate and permeate of the DRO module were taken throughout each experiment.

3.4.2.1 New control strategy for the saltwater tank

The control strategy for the saltwater tank during phase 2 is shown in Figure 3-5. The overflow system was replaced by the DRO module. The direction of the controller was reversed to decrease the conductivity when it rose above the setpoint value and the controller was changed to a PI-controller with a P-range of 1 mS/cm and an integration time of 300 seconds. The temperature was again manually controlled by increasing or decreasing the flow rate of the cooling water. The addition of the DRO module and the recycle stream resulted in the addition of another variable that should be controlled, namely the level in the saltwater tank. The level was manually controlled by opening or closing the valve on the retentate stream, thus increasing or decreasing the pressure inside the DRO module. A higher pressure resulted in an increased permeate flow rate and a decreased level in the saltwater tank and vice versa. The permeate flow rate and saltwater feed rate affects both the level and the concentration in the saltwater tank, making this a multiple-input-multiple-output (MIMO) control strategy.

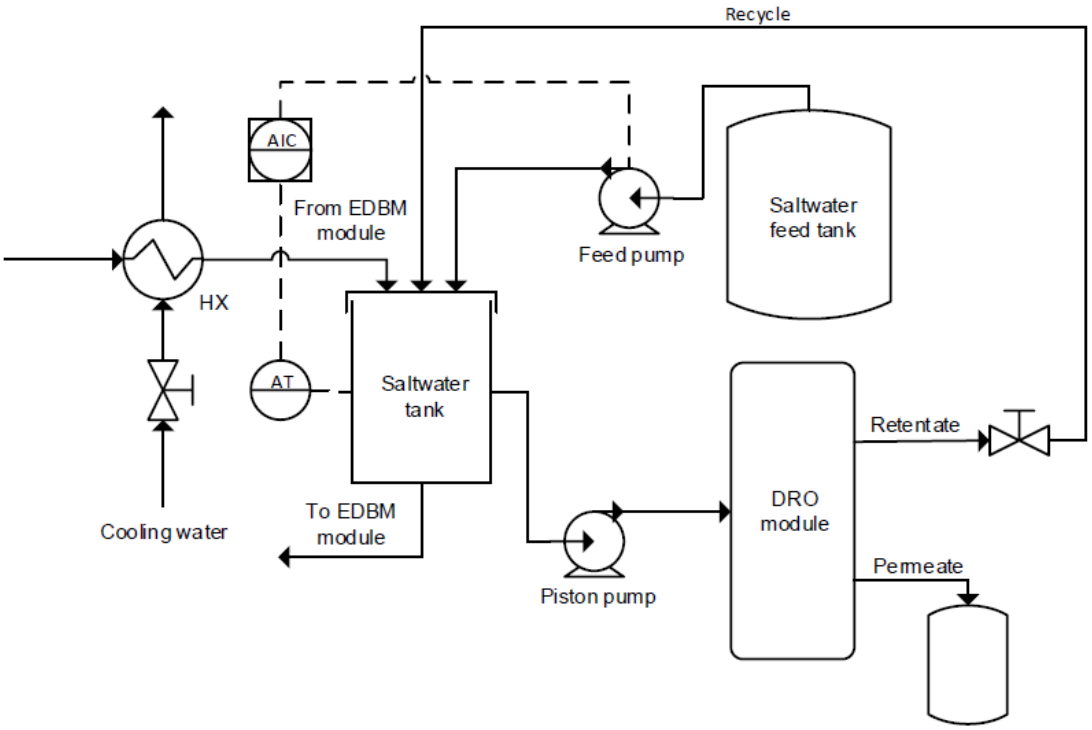

Figure 3-5: Schematic of the control strategy for the saltwater tank during phase 2

3.5 Analytical methods

The voltage and current, as well as the temperature and conductivity of the saltwater-, sodium hydroxide- and sulphuric acid tank, were recorded by the data logger every minute of each experiment. The samples taken were analysed for Na^+ and SO_4^{2-} content using inductively coupled plasma optical emission spectroscopy (ICP-OES) on an Agilant Technologies 700 series ICP. The pH of every sample was also tested using a Hanna HI8424 pH meter.

CHAPTER 4: RESULTS AND DISCUSSION

The experimental setup used and the experimental procedure followed was explained in Chapter 3. Chapter 4 focusses on the results obtained during the experimental phase of this study and the optimal conditions for EDBM-DRO operation is discussed.

4.1 Process control

The first objective was to design a robust control system for the process and to demonstrate its ability to maintain the process variables at the desired setpoint. The results of the control strategy discussed in Chapter 3 are shown in sections 4.1.1 – 4.1.2.

4.1.1 Temperature control

The temperature in the saltwater tank was maintained at its setpoint using a heat exchanger and cooling water. The temperature was manually controlled by increasing or decreasing the flow rate of cooling water through the heat exchanger. The temperature in the sodium hydroxide tank and the sulphuric acid tank was maintained at its setpoint via heat transfer to the saltwater channels inside the EDBM module. The control performance can be seen in Figure 4-1.

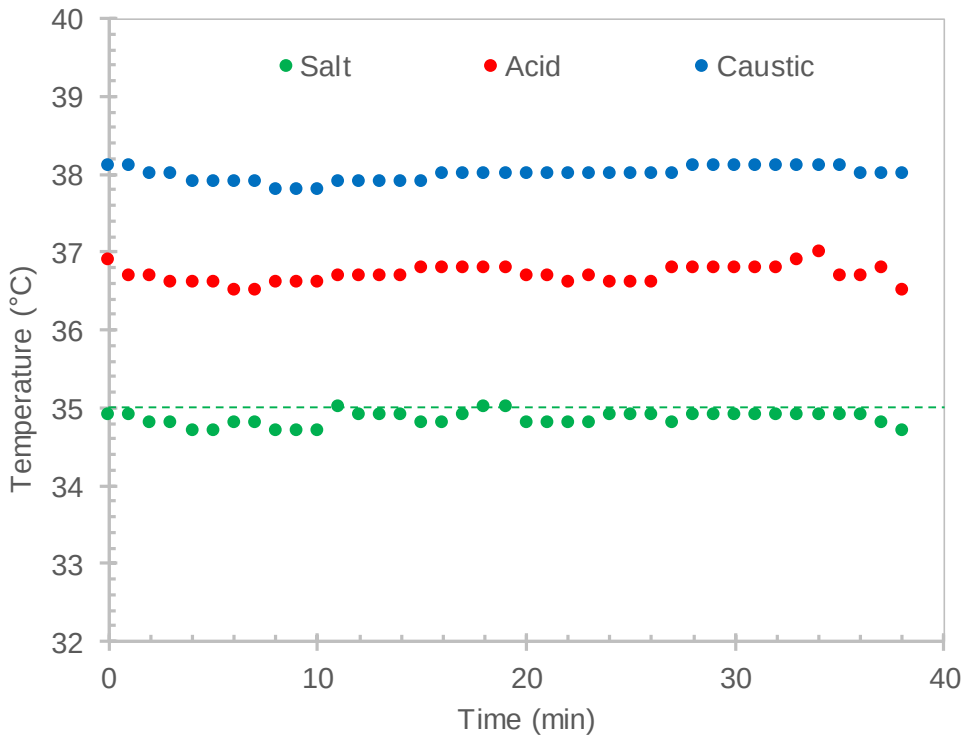

Figure 4-1: Temperatures in the saltwater, acid and caustic tanks throughout a 40-minute experiment.

The temperature in the saltwater tank deviated by a maximum of 0.3 °C from the setpoint of 35 °C throughout the experiment, indicated by the green dotted line in Figure 4-1. The temperatures

in the caustic and acid tank were 3 °C and 2 °C higher than the setpoint of 35 °C respectively. This temperature difference is sufficient to transfer the heat released in these channels by the salt splitting process. All temperatures were thus kept well below the 40 °C maximum.

4.1.2 Electrical conductivity control

The electrical conductivity in the caustic and acid tanks were set to 281 mS/cm and 191 mS/cm respectively, while the electrical conductivity setpoint of the saltwater tank depended on the experiment. In Figure 4-2, the setpoint of the saltwater tank is 91 mS/cm, which corresponds to a salt concentration of 100 g Na_2SO_4/L at 35 °C.

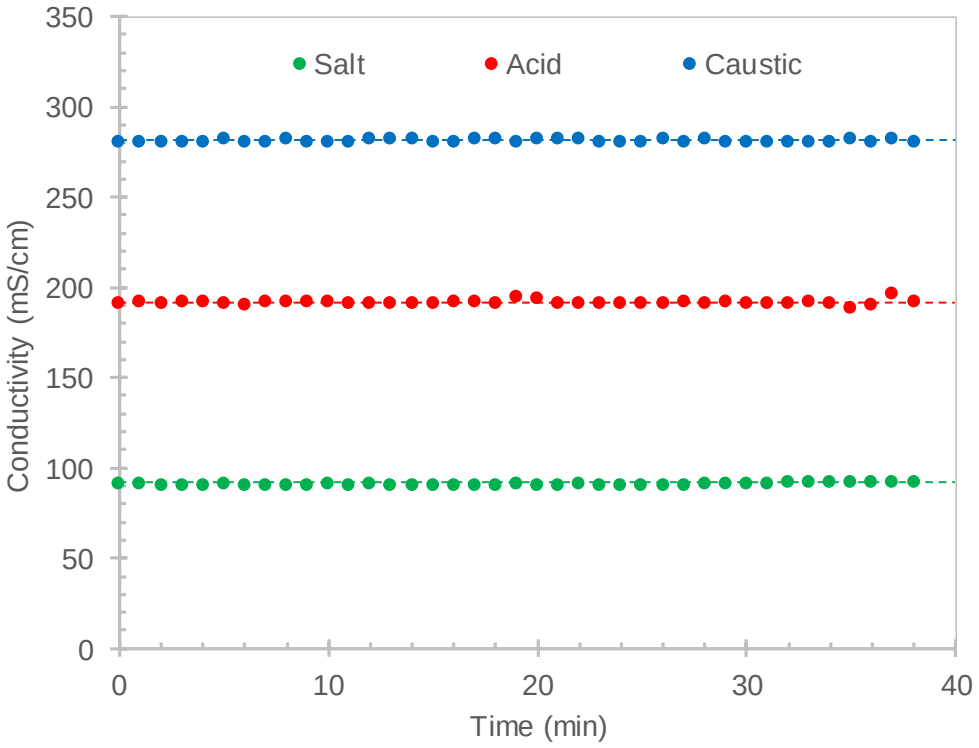

Figure 4-2: Electrical conductivity in the saltwater, acid and caustic tanks.

The electrical conductivity in the caustic, acid and saltwater tank had standard deviations of 0.49 mS/cm, 1.19 mS/cm and 0.64 mS/cm respectively. Figure 4-3 shows the setpoint tracking of the saltwater tank together with the corresponding mass change in the saltwater feed tank.

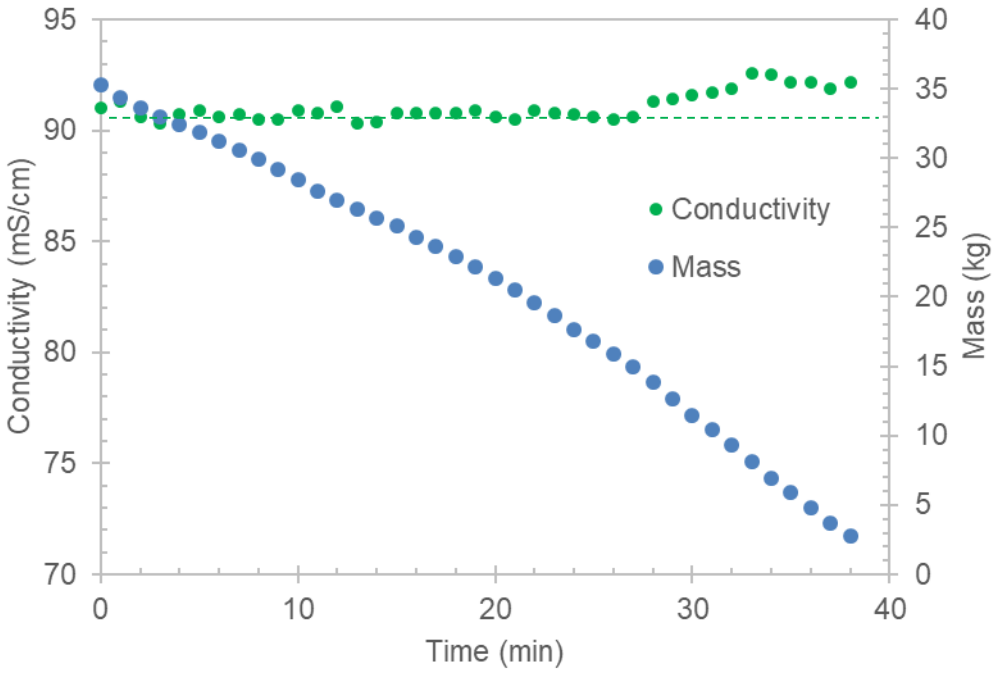

Figure 4-3: Setpoint tracking in the saltwater tank together with the corresponding mass change in the saltwater feed tank.

Figure 4-3 and Figure A - 1 in Appendix A, together with the known feed concentration of 49.06 g/L, can be used to find a saltwater feed rate of 48.54 L/h. This corresponds to a salt feed rate (SFR) of 2.38 kg/h.

4.2 Permeate flow rate tests

The permeability of the DRO module was evaluated for four cases: 100 g Na_2SO_4/L and 150 g Na_2SO_4/L each at neutral pH and pH of 2. Figure 4-4 shows that at neutral pH the osmotic pressure increases from 33 bar at 100 g Na_2SO_4/L to 49 bar at 150 g Na_2SO_4/L and it shows that the pH does not seem to have a significant effect on the osmotic pressure. Van't Hoff's equation can be used to determine the osmotic pressure of ideal solutions and is given by Equation (4-1).

$$\pi = i \cdot C \cdot R \cdot T \tag{4-1}$$

With π, the osmotic pressure (Pa), i the Van't Hoff's factor, a measure of the number of ions a solute will form when dissolved in water, C the molar concentration (mol/m^3), R the ideal gas constant (8.314 J/mol/K) and T the temperature (K) (Steele & Mills, 2021).

Osmotic pressures of 54 bar and 81 bar are calculated for solutions of 100 g Na_2SO_4/L and 150 g Na_2SO_4/L respectively. The substantially lower values found in the permeate flow rate tests is due to the non-ideality of high concentration solutions, where Na_2SO_4 do not fully dissociate into its ions (Atkins & de Paula, 2006).

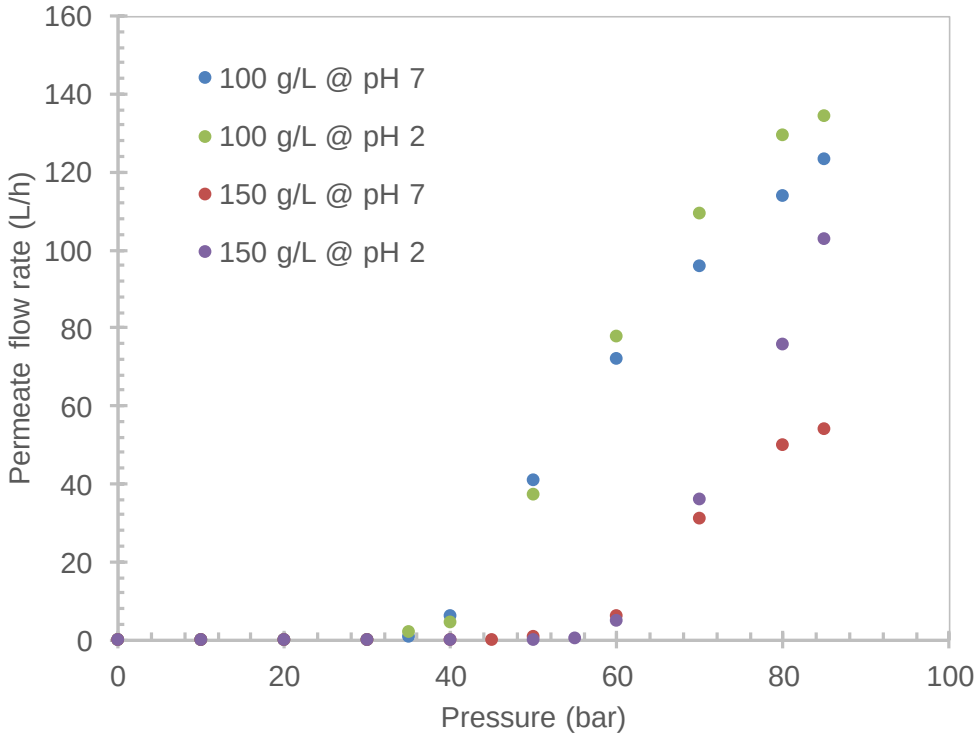

Figure 4-4: Permeate flow rate vs pressure for four cases

The pH of the permeate was also tested in the cases where the feed pH equalled 2. Figure 4-5 shows an increasing acid retention with an increase in pressure. This can be explained by a well-known phenomenon in reverse osmosis technology called membrane compaction. According to Stade et al (2015), the retention factor of a membrane can be positively impacted by compaction of a polymeric membrane, resulting in a denser membrane structure with increased hydrodynamic resistance. An increased pressure drop typically leads to a more pronounced effect of membrane compaction (Volkov, 2015).

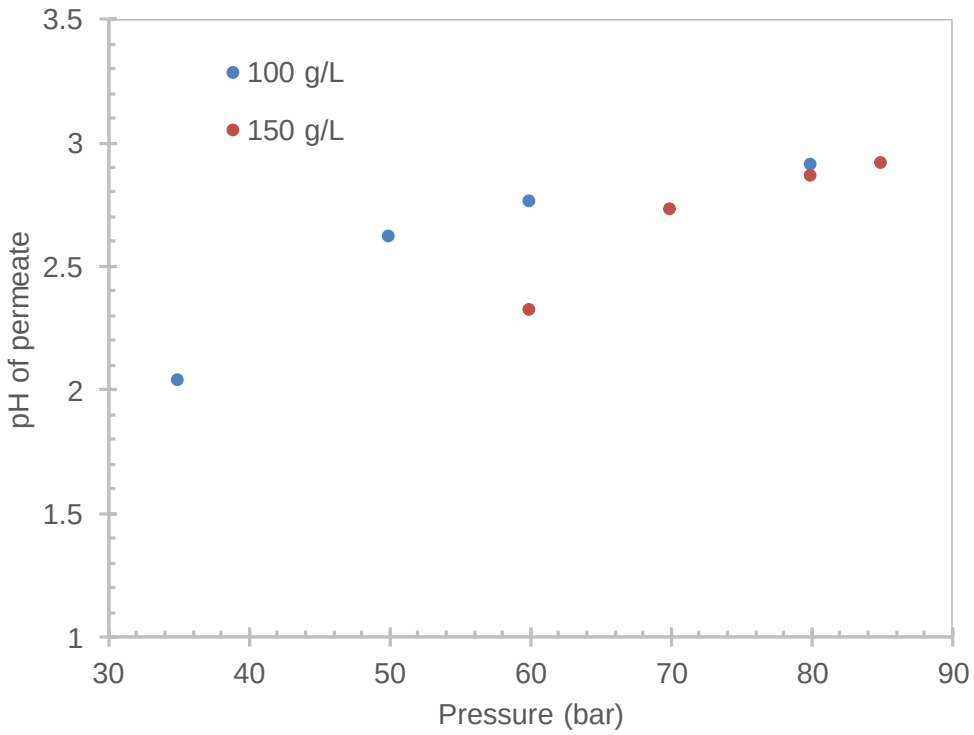

Figure 4-5: pH of permeate vs pressure

4.3 Effect of salt concentration

Increasing the salt, acid or caustic concentration in their respective tanks increase the electrical conductivity as seen in Figure 4-6. The overall electrical conductivity for the EDBM module, considering that all channels have the same gap width of 0.5 mm, can then be calculated using Equation (4-2).

$$EC_{ov} = \frac{3}{\frac{1}{EC_{Na_2SO_4}} + \frac{1}{EC_{NaOH}} + \frac{1}{EC_{H_2SO_4}}} \quad (4\text{-}2)$$

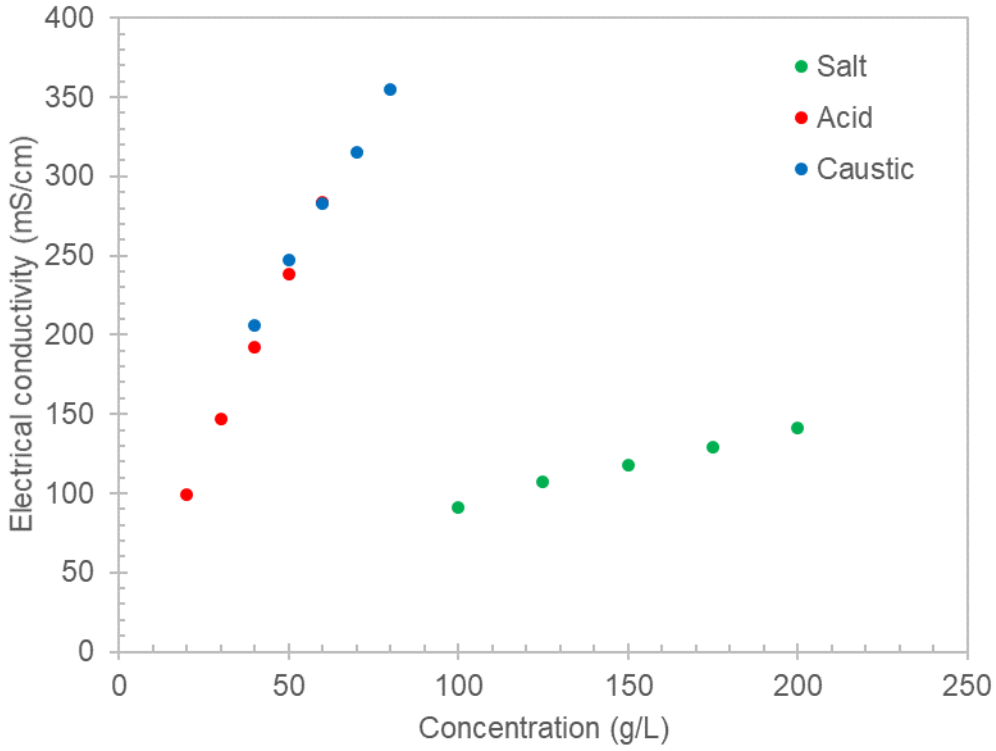

Figure 4-6: EC vs concentration at 35 °C

The salt concentration has a greater effect on the overall electrical conductivity as it has the highest resistance in this case of resistances in series and should thus be kept as high as possible to increase the overall electrical conductivity. This increase in the overall electrical conductivity corresponds to an increase in the specific salt splitting rate, specific caustic production rate (CPR) and specific acid production rate (APR) and a decrease in the specific energy consumption for sodium hydroxide as seen in Figure 4-7.

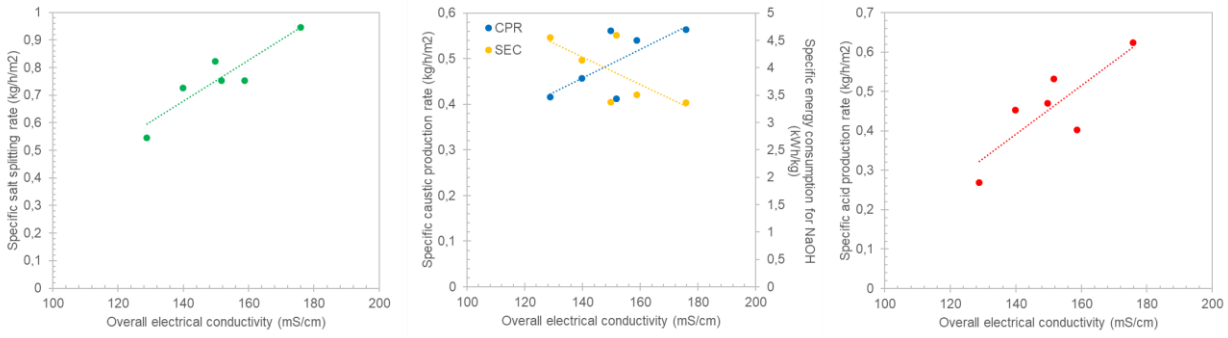

Figure 4-7: SSR (a), CPR and SEC (b) and APR (c) vs overall electrical conductivity

The conductivity of a solution, k (mS/cm), depends on the molar conductivity, Λ_m (mS/cm/mol/L), and the concentration of the electrolyte, C (mol/L) as seen in equation (4-3) (Atkins & de Paula, 2006):

$$k = \Lambda_m \cdot C \tag{4-3}$$

The molar conductivity is given by Kohlrausch's law:

$$\Lambda_m = \Lambda^\circ_m - K \cdot C^{\frac{1}{2}} \tag{4-4}$$

Where Λ°_m is the molar conductivity at infinite dilution and K is the Kohlrausch coefficient. Using equations (4-3) and (4-4), together with experimental data for the concentration vs. electrical conductivity of sodium sulphate solution at 35°C found in Table 4-1, a theoretical maximum electrical conductivity at a certain concentration can be determined.

Table 4-1: EC vs. concentration for sodium sulphate solutions at 35°C

Concentration (g/L)	Electrical conductivity (mS/cm)
100	91
125	107
150	118
175	129
200	141

The theoretical maximum electrical conductivity for sodium sulphate at 35°C is 165 mS/cm at a concentration of 350 g/L. The overall electrical conductivity of the system can thus be increased to a maximum value of 202 mS/cm, a 16% increase on the maximum overall electrical conductivity used during this study. Although the increased overall electrical conductivity can lead to a higher salt splitting rate and a lower specific energy consumption for sodium hydroxide, the higher sodium sulphate concentration will also lead to a higher osmotic pressure and thus higher energy usage by the DRO module due to the need for higher applied pressure.

4.4 Effect of temperature

The effect of temperature on various parameters is summarised in Table 4-2.

Table 4-2: Effect of temperature on EDBM performance

	20 °C	35°	Percentage change
Specific SSR ($kg/h/m^2$)	0.64	1.05	65.82
Specific CPR ($kg/h/m^2$)	0.39	0.56	44.34
Specific APR ($kg/h/m^2$)	0.41	0.76	85.97
SEC_{NaOH} (kWh/kg)	4.90	3.40	-30.66

The specific salt splitting rate, specific caustic production rate and specific acid production rate increased by 65.82%, 44.34% and 85.97% respectively and the specific energy consumption of sodium hydroxide decreased by 31% when the operating temperature increased from 20 °C to 35 °C. This is due to the higher electrical conductivity at higher temperatures as shown in Figure 4-8.

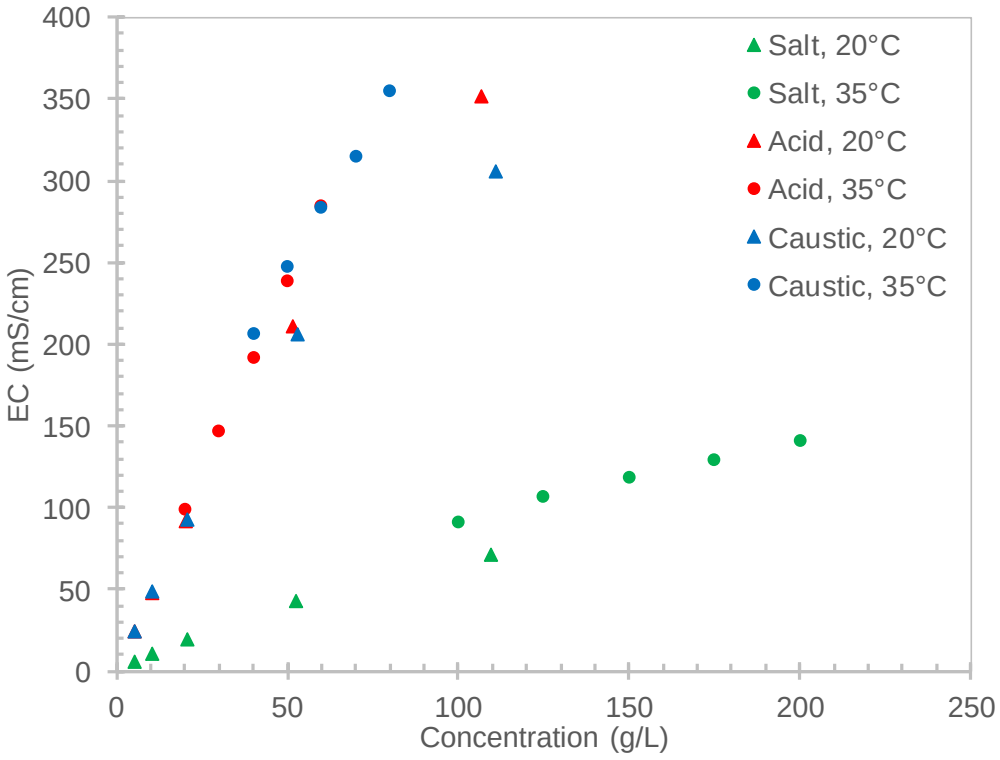

Figure 4-8: Effect of temperature on EC

The operating temperature was capped at 35 °C to protect the membranes of the EDBM module, however, limited studies have been done on the longevity of EDBM modules at elevated temperatures. A study should thus be done on the efficiency and longevity of the EDBM module at elevated temperatures to determine an optimal (cost) operating temperature.

4.5 Circulation flowrate dependence

A decrease in the concentration of a specific component near the boundary layer of a membrane due to selective transport through the membrane is termed concentration polarisation. A concentration profile similar to Figure 4-9 is formed when mass transfer resistance in the boundary layer dominates (Luis, 2018; Nikonenko *et al.*, 2017).

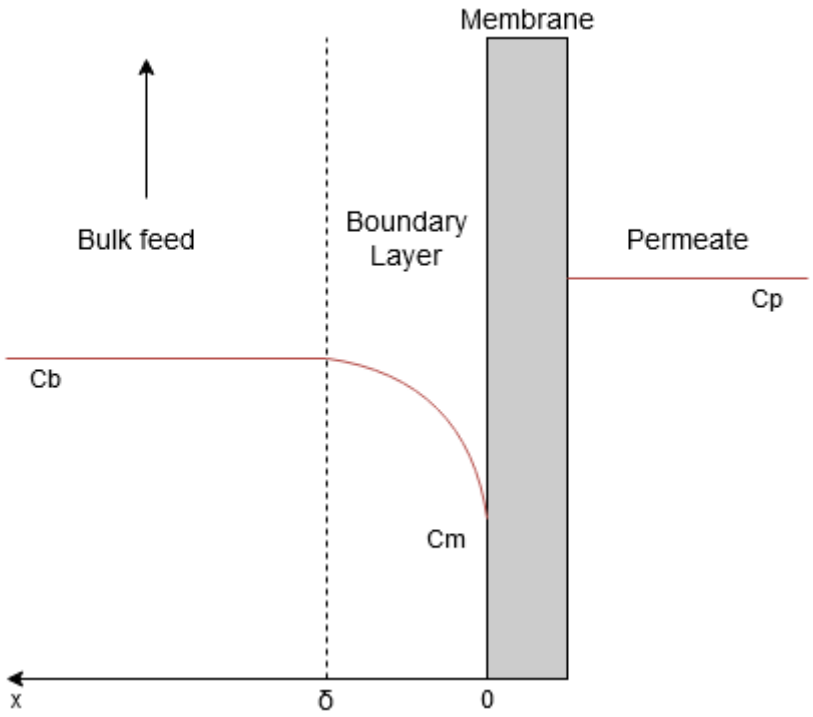

Figure 4-9: Schematic of concentration polarisation at the feed side (Luis, 2018)

Concentration polarisation negatively affects the separation process due to the higher resistance in the boundary layer. To reduce concentration polarisation, the flow rate of the solution can be increased, resulting in a decrease in the boundary layer thickness (Baker, 2012). Table 4-3 shows a 7.30% decrease in the specific salt splitting rate and a 1.73% decrease in the SEC_{NaOH} when doubling the flow rate of the electrolytes. The difference between the minimum obtainable 8.86 cm/s electrolyte superficial velocity and the maximum obtainable 17.4 cm/s electrolyte superficial

velocity is thus marginal, proving that mass transfer limitations become negligible at high flow rates.

Table 4-3: Effect of electrolyte flow rate on EDBM performance

	500 L/h	1000 L/h	Percentage change
Specific SSR ($kg/h/m^2$)	0.81	0.75	-7.30
Specific CPR ($kg/h/m^2$)	0.40	0.41	2.03
Specific APR ($kg/h/m^2$)	0.61	0.53	-13.44
SEC_{NaOH} (kWh/kg)	4.67	4.59	-1.73
Superficial velocity (cm/s)	8.68	17.4	100

4.6 Current- and power density dependence

Figure 4-10 shows how the specific rates depend on the power density for 100 g Na_2SO_4/L (91 mS/cm) and 150 g Na_2SO_4/L (121 mS/cm) in the salt vessel. For 100 g/L, a maximum specific salt splitting rate of 0.84 $kg/h/m^2$ is reached at a power density of 1.83 kW/m^2. This increases to 1.08 $kg/h/m^2$ at a power density of 1.76 kW/m^2 for 150 g/L.

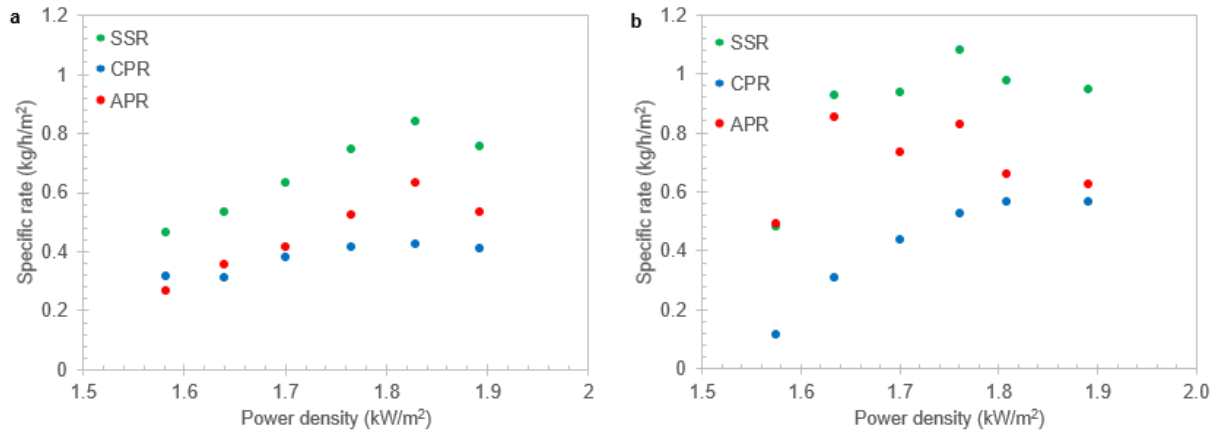

Figure 4-10: Specific rates vs current density for 91 mS/cm (a) and 121 mS/cm (b)

A minimum specific energy consumption of 4.28 kWh/kg is found at a power density of 1.77 kW/m^2 for 100 g/L and this is lowered to a specific energy consumption of 3.19 kWh/kg at a power density of 1.81 kW/m^2 for 150 g/L as seen in Figure 4-11.

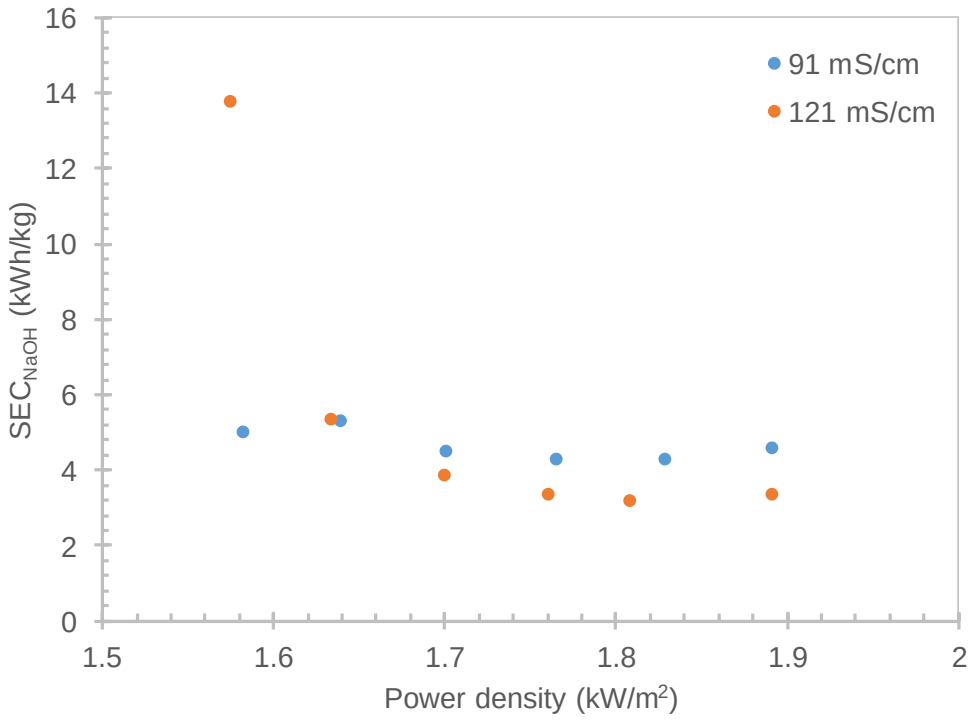

Figure 4-11: SEC$_{NaOH}$ vs power density

4.7 Cost estimation for the production of NaOH

The cost to produce 1 kg of sodium hydroxide can be calculated with Equation (4-5).

$$Cost_{NaOH} = \frac{\frac{Cost_{membrane}}{8000 \cdot LT_{membrane}} + \frac{Cost_{module}}{8000 \cdot LT_{module}}}{CPR} + Cost_{el} \cdot SEC_{NaOH} \quad (4\text{-}5)$$

The equipment cost and factors are listed in Table 4-4.

Table 4-4: Equipment cost and EDBM cost factors

	Value	Unit	Reference
Membrane cost	2500	€/m^2	(Wachs, 2020)
Membrane lifetime	2	year	(Tongwen, 2002)
Module cost	7500	€/m^2	(Wachs, 2020)
Module lifetime	5	year	(Tongwen, 2002)
Electricity cost	0.055	€/kWh	(Global Petrol Prices, 2020)
Operational	8000	h/year	(Tongwen, 2002)

Figure 4-12 shows a decrease in the sodium hydroxide production cost with an increasing power density. The optimal sodium hydroxide production cost of €0.78/kg is found at a power density of 1.81 kW/m^2, a sodium sulphate concentration of 150 g/L, an operating temperature of 35°C and an electrolyte flowrate of 1000 L/h. For comparison, according to Alibaba (2021), the market value of sodium hydroxide is €0.21/kg to €0.24/kg.

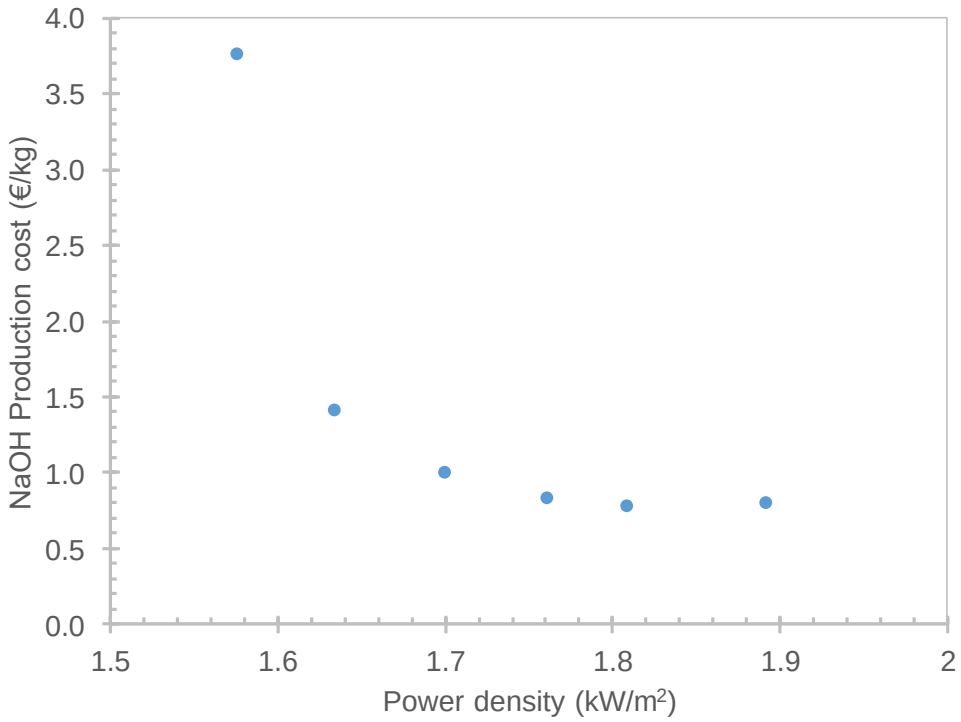

Figure 4-12: Sodium hydroxide production cost vs power density

4.8 Product compositions and purities

The EDBM-DRO produces three product streams: caustic, acid and permeate and has one reagent stream: saltwater. These streams were analysed by ICP and the results are given in Na^+ and SO_4^{2-} concentrations. In appendix B it is shown how this data is converted to NaOH and Na_2SO_4 concentrations as well as impurities. The results are summarised in Table 4-5.

Table 4-5: Average product compositions and impurities for the 91 mS/cm and 121 mS/cm case.

Product	NaOH (g/L)	H_2SO_4 (g/L)	Na_2SO_4 (g/L)	Impurity (wt%)
Caustic (91 mS/cm)	65.6	n.a.	7.00	9.6
Acid (91 mS/cm)	n.a.	54.1	30.0	35.7
Permeate (91 mS/cm)	n.a.	0.65	2.30	n.a.
Salt (91 mS/cm)	n.a.	10.2	89.0	10.3
Caustic (121 mS/cm)	67.7	n.a.	7.05	9.4
Acid (121 mS/cm)	n.a.	53.8	16.9	23.9
Permeate (121 mS/cm)	n.a.	0.41	2.07	n.a.
Salt (121 mS/cm)	n.a.	11.2	141.0	7.3

The caustic has an average free NaOH concentration of 66.5 g/L, which is above the target of 60 g/L. Due to the presence of 7.02 g Na_2SO_4/L, the caustic purity equals 90.5%. The acid has an average free H_2SO_4 concentration of 53.7 g/L, which is again well above the target of 40 g/L. The acid purity is 74% due to the presence of Na_2SO_4. The permeate for both cases was slightly acidic, with 97.4% and 98.5% of the salt removed from the 91 mS/cm and 121 mS/cm feed to the DRO. The concentration of sodium sulphate in the salt tanks was lower than the target in both cases due to the sulphuric acid impurity. The salt tank becomes slightly acidic, reaching a steady-state pH of 1.81, mainly due to proton transfer via the cation exchange membrane.

CHAPTER 5: CONCLUSIONS AND RECOMMENDATIONS

The results of the study and the optimal conditions for EDBM-DRO operation were discussed in Chapter 4. Chapter 5 concludes the study and highlights some recommendations for future studies on this subject.

5.1 Conclusions

The literature study highlighted the need for alternative ways to treat saltwater produced in base metal refineries and salt splitting by electrodialysis with bipolar membranes was proposed as an alternative to the current method, evaporative crystallisation.

The control strategy kept the concentrations, temperatures and tank levels at the desired setpoints for extended periods and thus proved the viability of continuous operation.

During the permeate flow rate tests, it was established that increasing the concentration of sodium sulphate in solution from 100 g/L to 150 g/L increased the osmotic pressure from 33 bar to 49 bar and that the presence of sulphuric acid did not have a significant effect on the osmotic pressure. Increasing the pressure inside the membrane resulted in increased acid retention due to a well-known phenomenon called membrane compaction.

The study showed that the salt splitting rate could be increased and the specific energy consumption for the production of sodium hydroxide could be lowered by increasing the salt concentration and temperature. Circulation flowrate tests showed that mass transfer limitations became negligible at the high flow rates used in this study. Increasing the power density generally resulted in an increased salt splitting rate and a decreased specific energy consumption for the production of sodium sulphate. A maximum salt splitting rate of 1.08 kg/h/m^2 at a power density of 1.76 kW/m^2 and a minimum specific energy consumption of 3.19 kWh/kg at a power density of 1.81 kW/m^2 was found.

The sodium hydroxide and sulphuric acid produced had concentrations of 66.5 g/L and 53.7 g/L and purities of 90.5% and 74% respectively, with sodium sulphate being the main impurity in both cases. The permeate from the disc reverse osmosis module was slightly acidic and 98% of the salt was removed from the feed stream.

The study proved that salt splitting technology can be integrated with disc reverse osmosis technology to produce sodium hydroxide, sulphuric acid and potable water from a concentrated sodium sulphate brine. The data generated during this study have been used to design a pilot plant with a salt splitting capacity of 100 kg/h and it will be operated 24/7 to test the longevity of the membranes in the electrodialysis with bipolar membranes module.

The lowest cost to produce sodium hydroxide, accounting for equipment cost, operational cost and electricity usage was found to be €0.78/kg at:

- A sodium sulphate concentration of 150 g/L (EC_{ov} = 176 mS/cm). This value needs to be optimised taking into account that higher salt concentrations will reduce the specific energy consumption to produce sodium hydroxide, but it will also require higher energy usage by the disc reverse osmosis module. An optimal salt concentration (in terms of economics) thus exists that is yet to be determined.
- An operating temperature of 35°C. This is the maximum temperature that is safe for the operation of the electrodialysis with bipolar membranes module.
- A power density of 1.81 kW/m^2.

5.2 Recommendations

- The operating temperature was capped at 35 °C to protect the membranes of the electrodialysis with bipolar membranes module, however, limited studies have been done on the longevity of electrodialysis with bipolar membranes modules at elevated temperatures. Increasing the temperature would increase the overall electrical conductivity and subsequently increase the salt splitting rate and decrease the specific energy consumption to produce sodium hydroxide, thus, increasing the temperature above 35°C might lead to lower sodium hydroxide production costs even at the expense of a shorter membrane lifetime. A study should thus be done on the efficiency and longevity of the electrodialysis with bipolar membranes module at elevated temperatures to determine an optimal (cost) operating temperature.
- The same argument can be used for the optimal concentrations of sodium hydroxide and sulphuric acid that come into contact with the membranes of the electrodialysis with bipolar membranes module. During this study, the concentrations of sodium hydroxide and sulphuric acid were fixed at the maximum recommended concentrations of 60 g/L and 40 g/L respectively. A study should thus also be done on the efficiency and longevity of the electrodialysis with bipolar membranes module at elevated sodium hydroxide and sulphuric acid concentrations to determine optimal (cost) operating concentrations.
- The study showed that the salt splitting rate could be increased and the specific energy consumption for the production of sodium hydroxide could be lowered by increasing the salt concentration. The theoretical maximum electrical conductivity for sodium sulphate at 35°C is 165 mS/cm at a concentration of 350 g/L, 200 g/L higher than the maximum salt concentration used in this study. The salt splitting rate could thus be increased by

concentrating the sodium sulphate solution even further. However, this would result in a much higher osmotic pressure and subsequently an increased energy cost for the disk reverse osmosis module. It is thus possible that an optimal (cost) concentration exists for sodium sulphate solution that is yet to be determined.

- The lowest production cost of sodium hydroxide established in this study was found to be €0.78/kg. To determine if this process is economical for a base metal refinery that produces sodium sulphate solution as a waste stream, all factors regarding the processing of sodium sulphate solution should be taken into account. A few things to consider are:
    - The produced sodium hydroxide and sulphuric acid must still be concentrated up to concentrations usable in the base metal refinery (± 200 g/L).
    - New sodium hydroxide and sulphuric acid need to be bought if the sodium salt is not split as opposed to recycling it to the base metal refinery.
    - The sodium sulphate solution cannot be discarded due to its high salinity and the processing costs of evaporative crystallisation should thus be taken into account.
    - If the salt solution is processed by evaporative crystallisation, a low-value salt is produced instead of high value caustic and acid that can be recycled to the base metal refinery. This salt can be sold but it can have a negative value, depending on the proximity of the base metal refinery to customers due to transportation costs.

BIBLIOGRAPHY

Alibaba. 2021. Sodium hydroxide price. https://www.alibaba.com/showroom/sodium-hydroxide-price.html Date of access: 1 March 2021.

Atkins, P. & de Paula, J. 2006. Atkins' Physical chemistry. 8. New York: Oxford University Press.

Baker, R.W. 2012. Membrane Technology and Applications. New York, UNITED KINGDOM: John Wiley & Sons, Incorporated.

Bernardes, A., Ferreira, J. & Rodrigues, M.A. 2014. Electrodialysis and water reuse: Novel approaches.

Carlberg, A. 2015. Modelling of Membrane in a Sodium Sulfate Electrochemical Splitting Cell.

Cole, S. & Ferron, C. 2002. A review of the beneficiation and extractive metallurgy of the platinum-group elements, highlighting recent process innovations. *SGS Minerals Services Technical Paper*, 3:1-43.

Crundwell, F., Moats, M., Ramachandran, V., Robinson, T. & Davenport, W.G. 2011. Extractive metallurgy of nickel, cobalt and platinum group metals: Elsevier.

Davis, S., Gray, G. & Kohl, P. 2008. Candidate membranes for the electrochemical salt-splitting of Sodium Sulfate. *Journal of Applied Electrochemistry*, 38:777-783.

Davis, T.A. 2000. MEMBRANE SEPARATIONS | Donnan Dialysis. *(In* Wilson, I.D., *ed.* Encyclopedia of Separation Science. Oxford: Academic Press. p. 1701-1707).

Department of mineral resources. 2017. Gross domestic product. https://www.dmr.gov.za/Portals/0/files/P04414thQuarter2017(1).pdf?ver=2018-03-09-063718-170 Date of access: 10 March 2020.

Donnan, F.G. 1924. The Theory of Membrane Equilibria. *Chemical Reviews*, 1(1):73-90.

Eisenberg, A. & Yeager, H.L. 1984. Perfluorinated ionomer membranes. American Chemical Society. *Reactive Polymers, Ion Exchangers, Sorbents*, 2(3):237-238.

El Cham, E., Alnouri, S., Mansour, F. & Al-Hindi, M. 2020. Design of end-of-pipe zero liquid discharge systems under variable operating parameters. *Journal of Cleaner Production*, 250:119569.

Engineering ToolBox. 2017. Density of aqueous solutions of inorganic sodium salts. https://www.engineeringtoolbox.com/density-aqueous-solution-inorganic-sodium-salt-concentration-d_1957.html Date of access: 10 March 2021

Fernández-Torres, M.J., Randall, D.G., Melamu, R. & von Blottnitz, H. 2012. A comparative life cycle assessment of eutectic freeze crystallisation and evaporative crystallisation for the treatment of saline wastewater. *Desalination*, 306:17-23.

Fritzmann, C., Löwenberg, J., Wintgens, T. & Melin, T. 2007. State-of-the-art of reverse osmosis desalination. *Desalination*, 216(1):1-76.

Global Petrol Prices. 2020. South Africa electricity prices. https://www.globalpetrolprices.com/South-Africa/electricity_prices/ Date of access: 1 March 2021.

Hagemann, J. & Pelser, M. 2016. Unlocking Rustenburg Base Metals Refiners sulphur removal section. *Journal of the Southern African Institute of Mining and Metallurgy*, 116:569-574.

Haggard, E., Sheridan, C. & Harding, K. 2015. Quantification of water usage at a South African platinum processing plant. *Water S.A*, 41:279.

HERA. 2006. Human and Environmental Risk Assessment on ingredients of Household Cleaning Products. Substance: Sodium Sulphate

Horvath, A.L. 1984. Handbook of Aqueous Electrolyte Solutions: Physical Properties, Estimation and Correlation Methods. New York: Wiley.

Huang, C. & Xu, T. 2006. Electrodialysis with Bipolar Membranes for Sustainable Development. *Environmental Science & Technology*, 40(17):5233-5243.

Kemperman, A.J.B. 2000. Handbook on Bipolar Membrane Technology: Twente University Press.

Lu, H., Wang, J., Wang, T., Wang, N., Bao, Y. & Hao, H. 2017. Crystallization techniques in wastewater treatment: An overview of applications. *Chemosphere*, 173:474-484.

Luis, P. 2018. Chapter 1 - Introduction. *(In* Luis, P., *ed.* Fundamental Modelling of Membrane Systems. Elsevier. p. 1-23).

Mani, K.N. 1991. Electrodialysis water splitting technology. *Journal of Membrane Science*, 58(2):117-138.

Nikonenko, V.V., Mareev, S.A., Pis'menskaya, N.D., Uzdenova, A.M., Kovalenko, A.V., Urtenov, M.K. & Pourcelly, G. 2017. Effect of electroconvection and its use in intensifying the mass transfer in electrodialysis (Review). *Russian Journal of Electrochemistry*, 53(10):1122-1144.

Ochieng, G.M., Seanego, E.S. & Nkwonta, O.I. 2010. Impacts of mining on water resources in South Africa: A review. *Scientific Research and Essays*, 5(22):3351-3357.

Panagopoulos, A., Haralambous, K.-J. & Loizidou, M. 2019. Desalination brine disposal methods and treatment technologies - A review. *Science of The Total Environment*, 693:133545.

Panda, R., Jha, M. & Pathak, D.D. 2018. Commercial Processes for the Extraction of Platinum Group Metals (PGMs). p. 119-130).

Pisarska, B., Mikołajczak, W., Jaroszek, H., Nowak, M., Dylewski, R. & Cichy, B. 2017. Processing of sodium sulphate solutions using the EED method: from a batch toward a continuous process. 19(1):54.

Raucq, D., Pourcelly, G. & Gavach, C. 1993. Production of sulphuric acid and caustic soda from sodium sulphate by electromembrane processes. Comparison between electro-electrodialysis and electrodialysis on bipolar membrane. *Desalination*, 91(2):163-175.

Saltworks. 2020. Next Generation Ultra High-Pressure Reverse Osmosis (UHP RO). https://www.saltworkstech.com/news/first-commercial-order-of-a-next-generation-ultra-high-pressure-reverse-osmosis-uhp-ro-industrial-system/ Date of access: 18 January 2021.

Sinha, P. & Kumar, R. 2019. A review on management of water resources in South Africa. *International Journal of Conservation Science*, 10(4).

Spiegler, K.S. & Laird, A.D.K. 1980. Principles of desalination. 2nd Edition. New York: Academic Press.

Stade, S., Kallioinen, M., Tuuva, T. & Mänttäri, M. 2015. Compaction and its effect on retention of ultrafiltration membranes at different temperatures. *Separation and Purification Technology*, 151.

Steele, E. & Mills, D. 2021. Osmotic Pressure: Definition & Formula. https://study.com/academy/lesson/osmotic-pressure-definition-formula-quiz.html Date of access: 2 February 2021.

Stilwell, L.C., Minnitt, R.C.A., Monson, T.D. & Kuhn, G. 2000. An input–output analysis of the impact of mining on the South African economy. *Resources Policy*, 26(1):17-30.

Strathmann, H. 2004. Assessment of Electrodialysis Water Desalination Process Costs.

Strathmann, H., Krol, J.J., Rapp, H.J. & Eigenberger, G. 1997. Limiting current density and water dissociation in bipolar membranes. *Journal of Membrane Science*, 125(1):123-142.

Tanaka, Y. 2015. Ion Exchange Membranes. Vol. 12: Elsevier.

Tongwen, X. 2002. Electrodialysis processes with bipolar membranes (EDBM) in environmental protection—a review. *Resources, Conservation and Recycling*, 37(1):1-22.

Tzanetakis, N., Taama, W.M. & Scott, K. 2002. Salt splitting in a three-compartment membrane electrolysis cell. *Filtration & Separation*, 39(3):30-38.

Van der Westhuizen, L. 2019. Recovery of acid and caustic from sodium sulphate rich base metal refinery effluent streams using bipolar membrane electrodialysis.

Volkov, A. 2015. Membrane Compaction. *(In* Drioli, E. & Giorno, L., *eds*. Encyclopedia of Membranes. Berlin, Heidelberg: Springer Berlin Heidelberg. p. 1-2).

FUMATECH, 2020. Operation manual of bipolar electro dialysis membrane module type FT-ED100-3-10

Zourmand, Z., Faridirad, F., Kasiri, N. & Mohammadi, T. 2015. Mass transfer modeling of desalination through an electrodialysis cell. *Desalination*, 359:41-51.

APPENDIX A: DENSITY CALCULATIONS

The experimental data used to draw Figure A - 1 is found in Table A - 1 and taken from The Engineering Toolbox (2017).

Table A - 1: Density data for NaOH at 20°C

Mass %	Density (kg/m^3)	Concentration (g/L)
0	1000	0
1	1007.1	10.071
5	1043.6	52.18
10	1090.5	109.05
20	1190.7	238.14

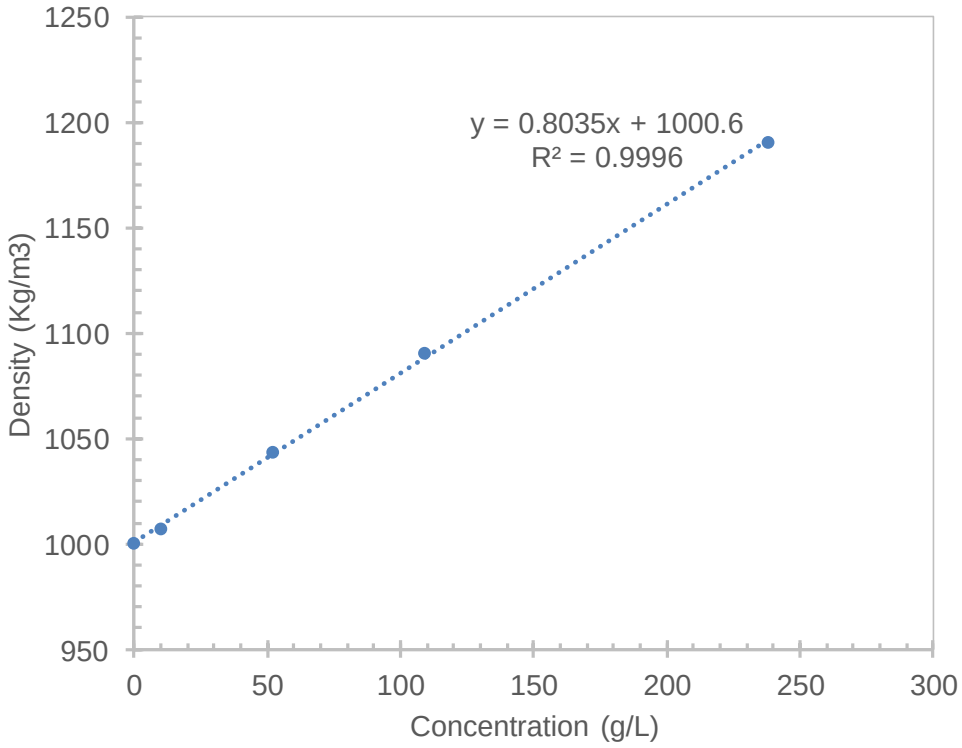

Figure A - 1: Density vs. concentration of a sodium sulphate solution at 25 °C.

APPENDIX B: IMPURITY CALCULATIONS

The EDBM-DRO produces three product streams: caustic, acid and permeate and has one reagent stream: salt. These streams were analysed by ICP-OES and the results are given in Na and S concentrations.

To convert S concentration to SO_4 concentration:

$$[SO_4] = [S] \cdot \frac{Mw_{SO_4}}{Mw_S} \tag{B-1}$$

For the acid, salt and permeate samples:

To calculate the Na_2SO_4 concentration:

$$[Na_2SO_4] = \frac{[Na] \cdot Mw_{Na_2SO_4}}{2 \cdot Mw_{Na}} \tag{B-2}$$

To calculate the H_2SO_4 concentration:

$$[H_2SO_4] = \frac{[SO_4] \cdot Mw_{H_2SO_4}}{Mw_{SO_4}} - \frac{[Na] \cdot Mw_{H_2SO_4}}{2 \cdot Mw_{Na}} \tag{B-3}$$

To calculate the impurities (permeate n.a.):

$$Imp = \frac{[Na_2SO_4]}{[Na_2SO_4] + [H_2SO_4]} \tag{B-4}$$

For the caustic samples:

To calculate the Na_2SO_4 concentration:

$$[Na_2SO_4] = \frac{[SO_4] \cdot Mw_{Na_2SO_4}}{Mw_{SO_4}} \tag{B-5}$$

To calculate the NaOH concentration:

$$[NaOH] = \frac{[Na] \cdot Mw_{NaOH}}{Mw_{Na}} - \frac{[SO_4] \cdot 2 \cdot Mw_{Na_2SO_4}}{Mw_{SO_4}} \quad \text{(B-6)}$$

To calculate the impurities:

$$Imp = \frac{[Na_2SO_4]}{[Na_2SO_4] + [NaOH]} \quad \text{(B-7)}$$